

$\gamma\delta$ T cells protect against lung fibrosis via IL-22

Philip L. Simonian,¹ Fabian Wehrmann,¹ Christina L. Roark,²
Willi K. Born,² Rebecca L. O'Brien,² and Andrew P. Fontenot^{1,2}

¹Department of Medicine, University of Colorado Denver, Aurora, CO 80045

²Integrated Department of Immunology, National Jewish Health, Denver, CO 80206

Inflammation-induced pulmonary fibrosis (PF) leads to irreversible loss of lung function and is a predictor of mortality in numerous lung diseases. Why some subjects with lung inflammation but not others develop PF is unclear. In a mouse model of hypersensitivity pneumonitis that progresses to lung fibrosis upon repeated exposure to the ubiquitous microorganism *Bacillus subtilis*, $\gamma\delta$ T cells expand in the lung and inhibit collagen deposition. We show that a subset of these $\gamma\delta$ cells represents the predominant source of the Th17 cytokine IL-22 in this model. Preventing expression of IL-22, either by mutating the aryl hydrocarbon receptor (AhR) or inhibiting AhR signaling, accelerated lung fibrosis. Direct blockade of IL-22 also enhanced collagen deposition in the lung, whereas administration of recombinant IL-22 inhibited lung fibrosis. Moreover, the presence of protective $\gamma\delta$ T cells and IL-22 diminished recruitment of CD4⁺ T cells to lung. These data reveal a protective pathway that involves the inhibition of $\alpha\beta$ T cells by regulatory IL-22-secreting $\gamma\delta$ T cells.

CORRESPONDENCE

Andrew Fontenot:
andrew.fontenot@ucdenver.edu

Abbreviations used: AhR, aryl hydrocarbon receptor; HP, hypersensitivity pneumonitis; PF, pulmonary fibrosis; TCDD, 2,3,7,8-Tetrachlorodibenzo-p-dioxin.

Hypersensitivity pneumonitis (HP) is an inflammatory lung disease that results from repeated inhalation of aerosolized antigens (Selman, 2003). The etiologic agents are composed of a wide variety of organic particles (e.g., mammalian and avian proteins, fungi, and bacteria) and certain small-molecular-weight volatile and nonvolatile chemical compounds. The severity of the inflammatory response depends on the nature of the antigen, the quantity and duration of exposure, and host-environment interactions (Selman, 2003). In chronically exposed patients, pulmonary fibrosis (PF) occurs in up to 41% of cases, resulting in irreversible pulmonary dysfunction and right heart failure (Mönkäre and Haahtela, 1987; Bourke et al., 1989; Lalancette et al., 1993; Yoshizawa et al., 1999). Importantly, lung fibrosis is an independent predictor of mortality in these patients, with a 5-yr mortality of 27% and a median survival of 13 yr (Vourlekis et al., 2004). Although PF is associated with numerous diffuse lung diseases, including autoimmune diseases (e.g., rheumatoid arthritis and systemic sclerosis), idiopathic PF, and sarcoidosis, its pathogenesis is poorly understood with few therapeutic options that arrest progression of fibrotic disease (Luzina et al., 2008).

$\gamma\delta$ T cells are a unique subset of lymphocytes whose function is poorly understood.

These cells, however, have been implicated in the regulation of the immune response generated against microbial pathogens and allergens (Born et al., 2007). The location of $\gamma\delta$ T cells in the subepithelium of alveolar and nonalveolar regions of the lung (Wands et al., 2005) suggests that these cells play an important role in the immune response directed against inhaled particles such as microbial pathogens (Nanno et al., 2007). We recently reported that V γ 6/V δ 1⁺ $\gamma\delta$ T cells isolated from the lung of mice chronically exposed to *Bacillus subtilis* express IL-17A (Simonian et al., 2009a). In this model of HP, C57BL/6 mice repeatedly treated with *B. subtilis* by nasal inhalation develop mononuclear infiltrates in the lung and PF that mimics the human disease (Simonian et al., 2006, 2009a; Barrera et al., 2008). Interestingly, large numbers of $\gamma\delta$ T cells, nearly all of which are V γ 6/V δ 1⁺, accumulate in the lung in response to *B. subtilis* and attenuate lung inflammation and fibrosis upon continued exposure to this ubiquitous environmental microorganism (Simonian et al., 2006). In the absence of $\gamma\delta$ T cells, TCR- $\delta^{-/-}$ mice treated with *B. subtilis* have accelerated lung fibrosis but similar levels of IL-17A to

Christina L. Roark's present address is Beacon Biotechnology, Aurora, CO 80045

© 2010 Simonian et al. This article is distributed under the terms of an Attribution-Noncommercial-Share Alike-No Mirror Sites license for the first six months after the publication date (see <http://www.rupress.org/terms>). After six months it is available under a Creative Commons License (Attribution-Noncommercial-Share Alike 3.0 Unported license, as described at <http://creativecommons.org/licenses/by-nc-sa/3.0/>).

those of WT mice as the result of a compensatory increase in IL-17A expression by CD4⁺ T cells. Conversely, IL-22 levels are reduced in TCR- $\delta^{-/-}$ mice (Simonian et al., 2009a), suggesting that IL-22 may be an important mechanism by which V γ 6/V δ 1⁺ $\gamma\delta$ T cells attenuate lung inflammation and fibrosis.

In this paper, we show that V γ 6/V δ 1⁺ $\gamma\delta$ T cells are the predominant cell type in the lung producing IL-22 in response to chronic *B. subtilis* exposure. In addition, these $\gamma\delta$ T cells differentially express IL-17A and IL-22, with IL-22 being expressed by a subset of IL-17F-producing V γ 6/V δ 1⁺ $\gamma\delta$ T cells. In the presence of the *d* allele of the aryl hydrocarbon receptor (AhR), AhR^{d/d} mice had reduced levels of IL-22 with accelerated collagen deposition in the lung. Administration of intratracheal recombinant mouse IL-22 (rIL-22) to *B. subtilis*-exposed AhR^{d/d} and TCR- $\delta^{-/-}$ mice significantly reduced lung inflammation and CD4⁺ T cell recruitment to lung and collagen deposition, suggesting that V γ 6/V δ 1⁺ $\gamma\delta$ T cells regulate lung inflammation and fibrosis through IL-22.

RESULTS

Lung V γ 6/V δ 1⁺ $\gamma\delta$ T cells express IL-22 in response to *B. subtilis*

We recently reported that WT C57BL/6 and homozygous V γ 6/V δ 1 transgenic (V γ 6^{+/+}) mice repeatedly exposed to *B. subtilis* have increased IL-22 levels in the lung compared with mice deficient in $\gamma\delta$ T cells (TCR- $\delta^{-/-}$ mice; Simonian et al., 2009a). To determine if $\gamma\delta$ T lymphocytes are an important source of IL-22, we performed intracellular cytokine staining on T cells isolated from the lung of WT C57BL/6, V γ 6^{+/+}, and TCR- $\delta^{-/-}$ mice. Gating on CD3⁺ $\gamma\delta$ ⁺ T cells, 6 and 9% of ex vivo V γ 6/V δ 1⁺ $\gamma\delta$ T cells isolated from the lung of WT C57BL/6 and V γ 6^{+/+} mice, respectively, express IL-22 after repeated exposure to *B. subtilis* for four consecutive weeks (Fig. 1 A). Consistent with a previous study (Martin et al., 2009), IL-22-secreting $\gamma\delta$ T cells also express CCR6 (not depicted). CD4⁺ T cells also produced IL-22 (Fig. 1 B), but the number of IL-22-expressing V γ 6/V δ 1⁺ $\gamma\delta$ T cells was significantly greater than CD4⁺ T cells in the lung of WT C57BL/6 and V γ 6^{+/+} mice (Fig. 1 C). Although TCR- $\delta^{-/-}$ mice had increased numbers of IL-22-expressing CD4⁺ T cells in the lung compared with WT C57BL/6 and V γ 6^{+/+} mice, levels of IL-22 were markedly diminished in the absence of $\gamma\delta$ T cells (Fig. 1 D). In addition, IL-22 levels were consistently lower in the lung of TCR- $\delta^{-/-}$ mice compared with V γ 6^{+/+} mice over the 4-wk time course and significantly reduced compared with WT C57BL/6 mice at 3 and 4 wk of repeated exposure to *B. subtilis* (Fig. 1 D). Collectively, these data suggest that although $\gamma\delta$ and CD4⁺ T cells both express IL-22, V γ 6/V δ 1⁺ $\gamma\delta$ T lymphocytes are the predominant source of IL-22 in the lung in response to repeated *B. subtilis* exposure.

Differential expression of IL-17A and IL-22 by V γ 6/V δ 1⁺ $\gamma\delta$ T cells

Recent studies show that $\gamma\delta$ T cells isolated from the peritoneal cavity after injection of heat-killed mycobacteria can

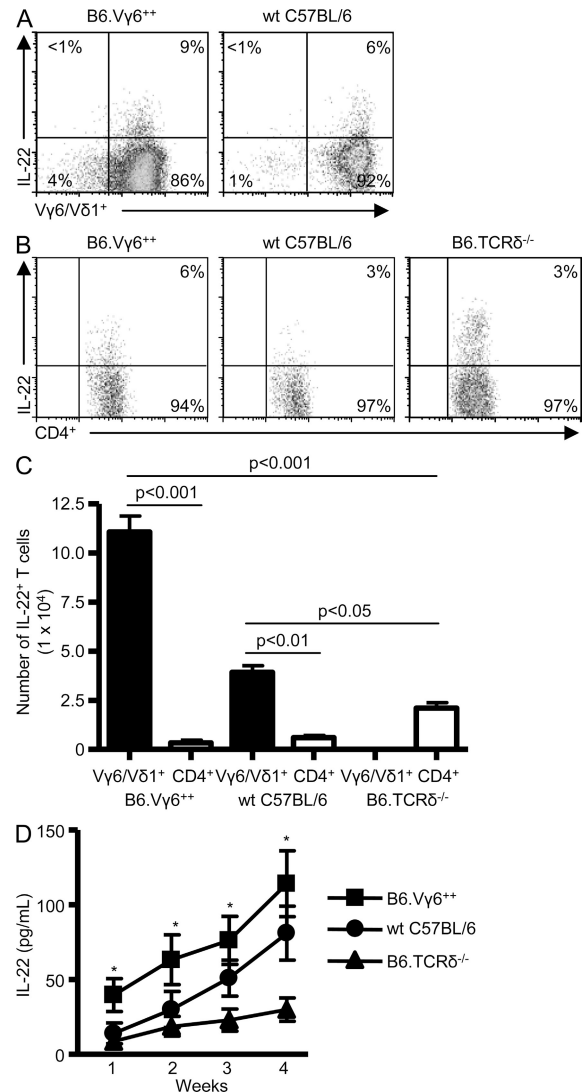


Figure 1. IL-22 expression by V γ 6/V δ 1⁺ $\gamma\delta$ and CD4⁺ T cells.

(A) Representative density plots of intracellular IL-22 expression in V γ 6/V δ 1⁺ $\gamma\delta$ T cells isolated from the lung of homozygous transgenic V γ 6/V δ 1 (B6.V γ 6^{+/+}) and WT C57BL/6 mice treated with *B. subtilis* for 4 wk. V γ 6/V δ 1⁺ $\gamma\delta$ T cells expressing IL-22 were selected from a bivariate dot plot of CD3⁺/CD8⁺ cells from the lymphocyte gate. The percentage of IL-22-expressing $\gamma\delta$ T cells is shown. (B) Representative density plots of intracellular IL-22 expression in CD4⁺ T cells isolated from the lung of B6.V γ 6^{+/+}, WT C57BL/6, and B6.TCR $\delta^{-/-}$ mice treated with *B. subtilis* for 4 wk. CD4⁺ T cells were selected from a bivariate dot plot of CD3⁺/side scatter cells from the lymphocyte gate. The percentage of CD3⁺CD4⁺ T cells expressing IL-22 is shown. (C) Absolute number of IL-22-expressing V γ 6/V δ 1⁺ $\gamma\delta$ or CD4⁺ T cells in the lung of B6.V γ 6^{+/+}, WT C57BL/6, and B6.TCR $\delta^{-/-}$ mice treated with *B. subtilis* for 4 wk. Data represent at least five individual mice per experiment from at least three separate experiments (mean \pm SD). (D) IL-22 concentration in the lung of mice treated with *B. subtilis*. Data represent at least five individual mice per experiment from at least three separate experiments (mean \pm SD). The asterisks denote a statistically significant ($P < 0.05$) difference in concentration of IL-22 in the lung of B6.V γ 6^{+/+} mice compared with B6.TCR $\delta^{-/-}$ mice.

express IL-22 (Martin et al., 2009). Similar to CD4⁺ T cells, $\gamma\delta$ T cells expressed either IL-17A alone or both IL-17A and IL-22 (Martin et al., 2009). In our model of HP and lung fibrosis induced by chronic exposure to *B. subtilis*, density plots of CD3⁺ $\gamma\delta$ ⁺ T cells revealed two distinct $\gamma\delta$ T cell populations (Fig. 2 A). Gating on the entire CD3⁺ $\gamma\delta$ ⁺ T cell population (Gate A) demonstrated that $\gamma\delta$ T cells isolated from the lung of V γ 6^{+/+} and WT C57BL/6 mice repeatedly exposed to *B. subtilis* differentially express IL-17A and IL-22 by intracellular cytokine staining (Fig. 2 A, top). In the representative examples shown in Fig. 2 A, 5% of CD3⁺ $\gamma\delta$ ⁺ T cells from the lung of WT C57BL/6 mice expressed IL-22, 11% expressed IL-17A, and very few cells expressed both cytokines. Conversely, $\gamma\delta$ T cells isolated from the spleen of WT C57BL/6 and V γ 6^{+/+} mice treated with *B. subtilis* did not express IL-22 (Fig. S1), suggesting a compartmentalized immune response in the lung directed against *B. subtilis*.

Gating on the brighter subset of $\gamma\delta$ T cells (Gate B), the percentage of IL-17A-expressing $\gamma\delta$ T cells increased with a concomitant decrease in the expression of IL-22 in both V γ 6^{+/+} and WT C57BL/6 mice (Fig. 2 A, middle), suggesting that this population of $\gamma\delta$ T cells more frequently expresses IL-17A. IL-17A expression was as high as 17% in this $\gamma\delta$ T cell subset with fewer $\gamma\delta$ T cells expressing IL-22 (2%). Gating on the less bright population of $\gamma\delta$ T cells (Gate C) resulted in an increased percentage of IL-22-expressing $\gamma\delta$ T cells, with as many as 12% of this subset producing IL-22, whereas fewer $\gamma\delta$ T cells expressed IL-17A (Fig. 2 A, bottom). Overall, the number of IL-17A-expressing $\gamma\delta$ T cells was markedly increased with a concomitant decrease in IL-22 expression in Gate B, whereas IL-22-expressing $\gamma\delta$ T lymphocyte numbers were significantly increased in Gate C (Fig. 2 B). Because the vast majority of $\gamma\delta$ T cells accumulating in the lung in response to *B. subtilis* express the V γ 6/V δ 1 TCR (Fig. 1 A; Simonian et al., 2006), these data demonstrate that V γ 6/V δ 1⁺ $\gamma\delta$ T cells differentially express IL-17A and IL-22 in response to repeated exposure to *B. subtilis*, suggesting the possibility that subsets of V γ 6/V δ 1⁺ $\gamma\delta$ T cells may have distinct functional capabilities.

Differential expression of IL-17A and IL-17F by V γ 6/V δ 1⁺ $\gamma\delta$ T cells

In addition to IL-17A, IL-17F was detected in the lung of WT C57BL/6, V γ 6^{+/+}, and TCR- δ ^{-/-} mice after repeated exposure to *B. subtilis* for four consecutive weeks (Fig. 3 A). As shown in Fig. 3 A, TCR- δ ^{-/-} mice have a twofold increased level of IL-17F in the lung compared with WT C57BL/6 mice and a 1.6-fold increase compared with V γ 6^{+/+} mice. Gating on CD3⁺CD4⁺ T cells, CD4⁺ T cells from the lung of TCR- δ ^{-/-} mice treated with *B. subtilis* differentially expressed IL-17A and IL-17F (Fig. 3 B). Unlike IL-17A, however, CD4⁺ T cells expressed high levels of IL-17F even in the presence of $\gamma\delta$ T cells in both WT C57BL/6 and V γ 6^{+/+} mice (Fig. 3 B). In addition, the absolute number of both IL-17F- and IL-17A-expressing CD4⁺ T cells was increased in the lung of TCR- δ ^{-/-} mice compared with WT

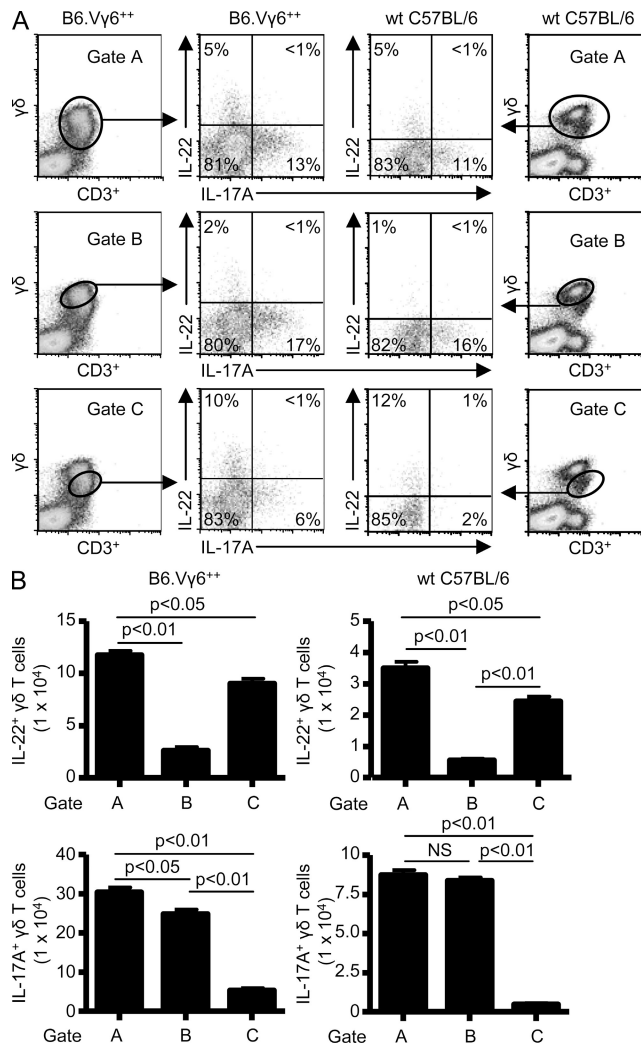


Figure 2. Differential expression of IL-22 and IL-17A by V γ 6/V δ 1⁺ $\gamma\delta$ T cells. (A) Representative density plots of intracellular IL-22 and IL-17A expression in $\gamma\delta$ T cells isolated from the lung of WT C57BL/6 and B6.V γ 6^{+/+} mice treated with *B. subtilis* for 4 wk. $\gamma\delta$ T cells expressing IL-17A or IL-22 were selected from a bivariate dot plot of CD3⁺/CD8⁺ cells from the lymphocyte gate. The percentage of $\gamma\delta$ T cells expressing either IL-17A or IL-22 is shown in each quadrant of the density plot. (B) Absolute number of IL-22- or IL-17A-expressing $\gamma\delta$ T cells in the lung of B6.V γ 6^{+/+} and WT C57BL/6 treated with *B. subtilis* for 4 wk using different gating strategies labeled A, B, or C. Data represent at least five individual mice per experiment from at least three separate experiments (mean \pm SD). NS, not significant. P > 0.05.

C57BL/6 and V γ 6^{+/+} mice (Fig. 3 C). Importantly, microbial elimination was similar in all three strains of mice (Simonian et al., 2009a).

As shown in Fig. 3 D, V γ 6/V δ 1⁺ $\gamma\delta$ T cells also differentially express IL-17A and IL-17F, with the majority of IL-17F expression identified in the less bright population of $\gamma\delta$ T cells (Fig. 3 D, Gate C, middle), similar to IL-22. As many as 48 and 44% of $\gamma\delta$ T cells isolated from the lung of *B. subtilis*-treated V γ 6^{+/+} mice and WT C57BL/6 mice, respectively, expressed IL-17F (Fig. 3 D, Gate A, top). In addition, gating

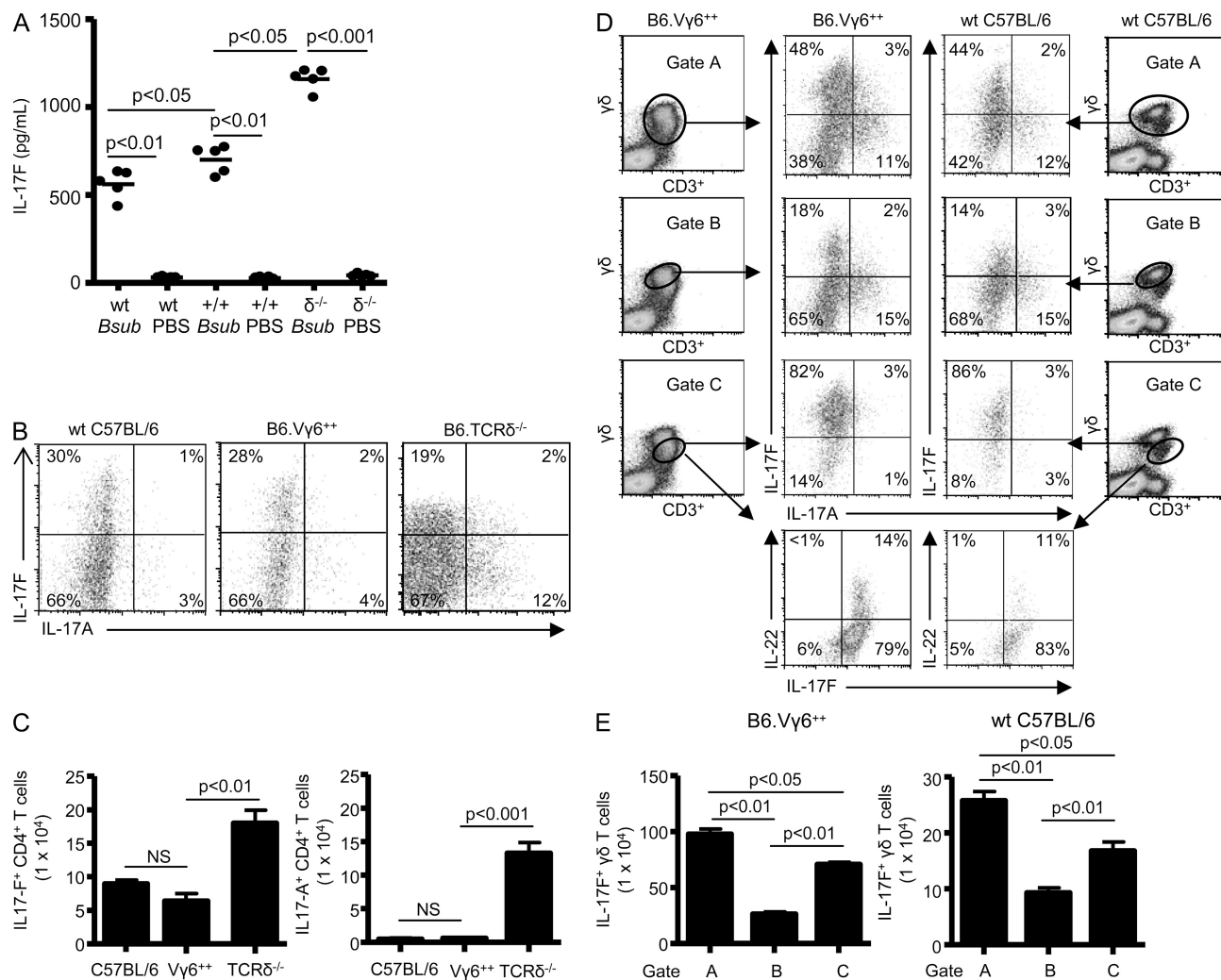


Figure 3. Differential expression of IL-17F and IL-17A by Vγ6/Vδ1⁺ γδ T cells. (A) IL-17F concentration in lung homogenates was analyzed by ELISA from WT C57BL/6 (wt), B6.Vγ6^{+/+} (+/+), and B6.TCRδ^{-/-} ($\delta^{-/-}$) mice treated with either *B. subtilis* or PBS for 4 wk. The mean is shown as a solid line. Data are compiled from five individual mice from at least two separate experiments. (B) Representative density plots of intracellular IL-17F and IL-17A expression in CD4⁺ T cells isolated from the lung of WT C57BL/6, B6.Vγ6^{+/+}, and B6.TCRδ^{-/-} mice treated with *B. subtilis* for 4 wk. CD4⁺ T cells that express IL-17F and IL-17A were selected from a bivariate dot plot of CD3⁺/CD4⁺-expressing cells in the lymphocyte gate. The percentage of CD4⁺ T cells expressing IL-17A or IL-17F is shown in each quadrant of the density plot. (C) Absolute number of IL-17A- or IL-17F-expressing CD4⁺ T cells in the lung of WT C57BL/6, B6.Vγ6^{+/+}, and B6.TCRδ^{-/-} mice treated with *B. subtilis* for 4 wk. Data represent at least five individual mice per experiment from at least three separate experiments (mean ± SD). (D) Representative density plots of intracellular IL-17F and IL-17A expression in γδ T cells isolated from the lung of WT C57BL/6 and B6.Vγ6^{+/+} mice treated with *B. subtilis* for 4 wk. γδ T cells expressing IL-17A, IL-17F, or IL-22 were selected from a bivariate dot plot of CD3⁺/CD4⁺ cells from the lymphocyte gate. The percentage of γδ T cells expressing IL-17A, IL-17F, or IL-22 is shown in each quadrant of the density plot. (E) Absolute number of IL-17F-expressing γδ T cells in the lung of B6.Vγ6^{+/+} and WT C57BL/6 treated with *B. subtilis* for 4 wk using different gating strategies labeled A, B, or C. Data represent at least five individual mice per experiment from at least three separate experiments (mean ± SD).

on the less bright population of γδ T cells confirmed dual expression of IL-22 and IL-17F by γδ T cells isolated from the lung of both Vγ6^{+/+} mice (14%) and WT C57BL/6 (11%; Fig. 3 D, Gate C, bottom). In addition, numbers of IL-17A-expressing γδ T cells were markedly increased with a concomitant decrease in IL-17F expression in Gate B, whereas IL-17F-expressing γδ T lymphocyte numbers were increased in Gate C (Fig. 3 E). These findings demonstrate that in response to *B. subtilis*, both γδ and CD4⁺ T cells differentially express IL-17A and IL-17F, with IL-22 expression

identified in a subset of IL-17F-expressing Vγ6/Vδ1⁺ γδ T lymphocytes.

Decreased expression of IL-22 in AhR^{d/d} mice repeatedly exposed to *B. subtilis*

Recent studies suggest that IL-22 expression requires the presence of AhR in CD4⁺ and γδ T cells (Veldhoen et al., 2008; Martin et al., 2009). To determine if IL-22 production was affected by expression of the *d* allele on the C57BL/6 background in this model, we treated AhR^{d/d} mice with

B. subtilis. The *d* allele codes for an AHR protein with reduced affinity for known ligands as a result of mutations in its ligand-binding site (Okey et al., 1989). As shown in Fig. 4 A, AhR^{d/d} mice had decreased levels of IL-22 in the lung compared with WT C57BL/6 mice treated in an identical fashion with *B. subtilis* for 4 wk. Levels of IL-17A and IL-17F, however, were similar in the lung of *B. subtilis*-treated WT C57BL/6 and AhR^{d/d} mice (Fig. 4 A). As shown in Fig. 4 B, $\gamma\delta$ T cells isolated from the lung of *B. subtilis*-treated AhR^{d/d} mice had reduced expression of IL-22 compared with WT C57BL/6 mice. In contrast, $\gamma\delta$ T cells maintained the capacity to express IL-17A as compared with WT C57BL/6 mice treated in an identical fashion (Fig. 4 B). CD4⁺ T cells did not express significant levels of either IL-22 or IL-17A (Fig. 4 B). $\gamma\delta$ and CD4⁺ T cells continued to express IL-17F at levels

that were not significantly different than those of cells from *B. subtilis*-treated WT C57BL/6 mice (Fig. 4, A and B). Overall, the number of IL-22-expressing $\gamma\delta$ T cells was decreased in the lung of AhR^{d/d} mice compared with WT C57BL/6 mice repeatedly exposed to *B. subtilis* in an identical manner, whereas numbers of IL-17A- and IL-17F-expressing $\gamma\delta$ T cells were unaffected (Fig. 4 C).

To determine whether decreased expression of IL-22 by V γ 6/V δ 1⁺ $\gamma\delta$ T cells affects *B. subtilis*-induced lung fibrosis, AhR^{d/d} mice treated with *B. subtilis* for four consecutive weeks were analyzed with Masson trichrome staining. As shown in Fig. 5 A, AhR^{d/d} mice developed mononuclear infiltrates and collagen deposition in a peribronchovascular distribution similar to WT C57BL/6 mice treated in an identical fashion. We have previously shown that TCR- $\delta^{-/-}$ mice develop

significantly increased lung fibrosis after *B. subtilis* exposure and are included for comparison (Simonian et al., 2009a). By quantitative analysis using Sirius red, AhR^{d/d} mice develop accelerated lung fibrosis with a 1.4-fold increased collagen content in the lung compared with *B. subtilis*-treated WT C57BL/6 mice ($P < 0.05$) and a nearly fourfold increase in collagen deposition compared with PBS-treated control animals ($P < 0.001$; Fig. 5 B). In addition, collagen deposition in the lungs of AhR^{d/d} mice at 4 wk of repeated exposure to *B. subtilis* was similar to the exaggerated fibrotic response seen in TCR- $\delta^{-/-}$ mice

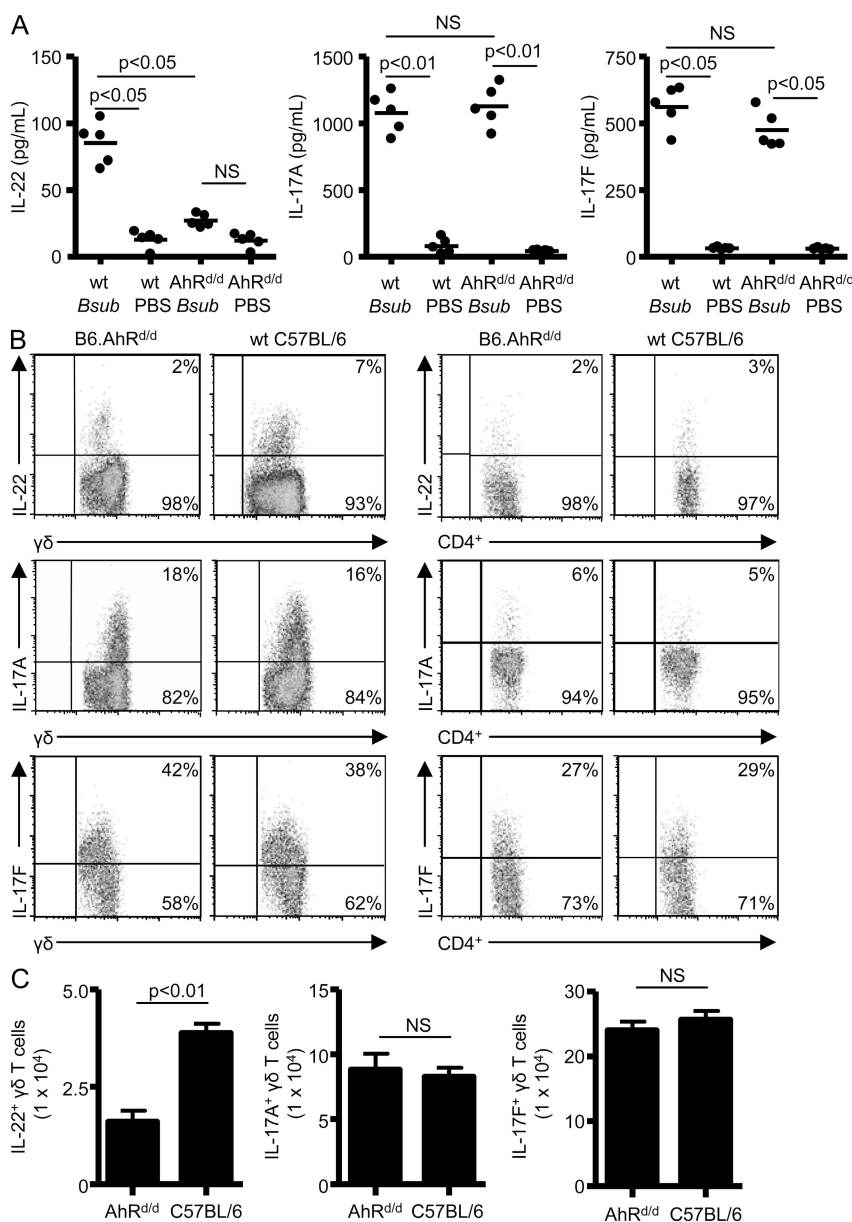


Figure 4. $\gamma\delta$ T cells from B6.AhR^{d/d} mice have reduced IL-22 expression. (A) Cytokines from supernatants of lung homogenates were analyzed by ELISA from WT C57BL/6 (wt) and B6.AhR^{d/d} mice treated with either *B. subtilis* or PBS for 4 wk. The mean is shown as a solid line. Data are compiled from five individual mice from at least two separate experiments. (B) Representative density plots of intracellular IL-22, IL-17A, and IL-17F expression in $\gamma\delta$ and CD4⁺ T cells isolated from the lung of B6.AhR^{d/d} mice treated with *B. subtilis* for 4 wk. $\gamma\delta$ T cells expressing IL-22, IL-17A, or IL-17F were selected from a bivariate dot plot of CD3⁺/CD8⁺ cells from the lymphocyte gate. CD4⁺ T cells that express IL-22, IL-17A, and IL-17F were selected from a bivariate dot plot of CD3⁺/side scatter-expressing cells in the lymphocyte gate. The percentage of T cells expressing IL-22, IL-17A, or IL-17F is shown in the top right quadrant of the density plot. Data are representative of at least five individual mice per experiment from at least three separate experiments. (C) Absolute number of IL-22-, IL-17A-, and IL-17F-expressing $\gamma\delta$ T cells in the lung of B6.AhR^{d/d} and WT C57BL/6 mice treated with *B. subtilis* for 4 wk. Data represent five individual mice per experiment from at least three separate experiments (mean \pm SD). NS, not significant. $P > 0.05$.

(Simonian et al., 2009a). Collectively, these findings suggest that $V\gamma 6/V\delta 1^+ \gamma\delta$ T cells protect against lung fibrosis through expression of IL-22.

Recombinant IL-22 decreases lung inflammation and fibrosis in $AhR^{d/d}$ and $TCR-\delta^{-/-}$ mice

To confirm that IL-22 protects against *B. subtilis*-induced lung inflammation and fibrosis, we treated mice with decreased IL-22 production (i.e., $AhR^{d/d}$ and $TCR-\delta^{-/-}$ mice) with intratracheal rIL-22 (100 pg and 100 ng) in combination with *B. subtilis* for 3 d each week for four consecutive weeks. As shown in Fig. 6 A, total cells and lymphocytes were significantly decreased in the lung of $AhR^{d/d}$ and $TCR-\delta^{-/-}$

mice treated with intratracheal rIL-22 and *B. subtilis* compared with control mice exposed to vehicle and *B. subtilis*. In addition, no significant changes in the number of total lung cells or lymphocytes in WT C57BL/6 mice were seen (Fig. S2). There was no significant change in the number of $\gamma\delta$ T cells in the lung of both WT C57BL/6 and $AhR^{d/d}$ mice treated with rIL-22 and *B. subtilis* (unpublished data). Conversely, $CD4^+$ T cells were significantly decreased in WT C57BL/6, $AhR^{d/d}$, and $TCR-\delta^{-/-}$ mice that received rIL-22 (Fig. 6 B), whereas treatment with rIL-22 alone had no effect on lung inflammation (not depicted).

Masson trichrome staining of lungs of $AhR^{d/d}$ and $TCR-\delta^{-/-}$ mice treated with *B. subtilis* and rIL-22 showed reduced mononuclear cell infiltrates and collagen deposition in a peribronchovascular distribution (Fig. 6 C). Using Sirius red colorimetric assay for collagen quantification, $AhR^{d/d}$ and $TCR-\delta^{-/-}$ mice that received intratracheal rIL-22 had decreased levels of collagen deposition in the lung compared with mice treated with *B. subtilis* alone. For example, there was a 2- and 1.5-fold decrease in collagen deposition in $AhR^{d/d}$ mice treated with 100 ng and 100 pg of rIL-22, respectively, compared with mice treated with *B. subtilis* alone (Fig. 6 D). $TCR-\delta^{-/-}$ mice also had a significant decrease in collagen deposition in the lung with a 1.6- and 1.3-fold decrease in collagen content in the lung of mice treated with 100 ng and 100 pg of rIL-22, respectively, compared with $TCR-\delta^{-/-}$ mice exposed to *B. subtilis* alone (Fig. 6 D). WT C57BL/6 treated with the higher concentration of rIL-22 (100 ng) had decreased collagen deposition compared with *B. subtilis* treatment alone, whereas $V\gamma 6^{+/+}$ mice, which have higher levels of IL-22 in the lung throughout the course of *B. subtilis* exposure (Fig. 1 D), did not have any additional decrease in lung fibrosis at either dose of rIL-22 (Fig. 6 D). In combination, these data demonstrate that exogenous rIL-22 is capable of modulating lung inflammation and fibrosis induced by chronic exposure to *B. subtilis*.

Inhibition of IL-22 expression increases lung inflammation and fibrosis

We next investigated whether inhibition of AhR signaling in $V\gamma 6/V\delta 1^+ \gamma\delta$ T cells would reduce IL-22 expression and accelerate the *B. subtilis*-induced inflammatory and fibrotic process. Because $V\gamma 6^{+/+}$ mice have increased levels of IL-22 in the lung and develop significantly less inflammation and fibrosis, we treated these mice with a chemical inhibitor of AhR, CH-223191. CH-223191 is a novel chemical compound that potently inhibits AhR-dependent transcription induced by 2,3,7,8-Tetrachlorodibenzo-p-dioxin (TCDD; Kim et al., 2006). In addition, CH-223191 has been shown to block binding of TCDD to AhR and inhibit TCDD-mediated nuclear translocation and DNA binding of AhR, thus preventing expression of target genes of AhR without detectable AhR agonist activity (Kim et al., 2006).

$V\gamma 6^{+/+}$ mice were treated with *B. subtilis* and either 10 mM or 10 μ M of CH-223191 for three consecutive days each week for four consecutive weeks. As shown in Fig. 7 A,

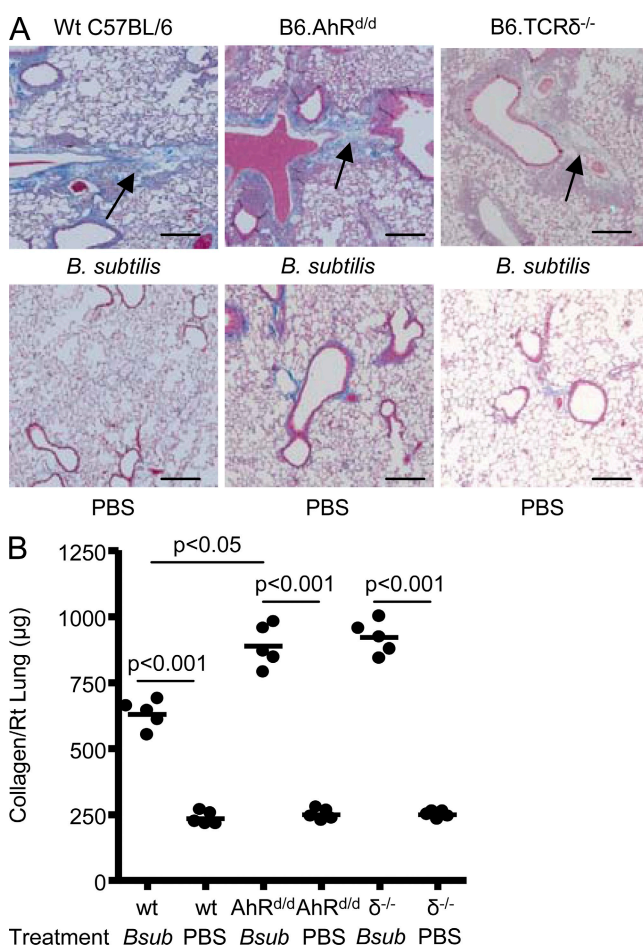


Figure 5. Defective AhR signaling accelerates lung fibrosis.

(A) Representative Masson's trichrome staining of lungs from WT C57BL/6, B6.AhR^{d/d}, and B6.TCRδ^{-/-} mice repeatedly treated with *B. subtilis* or PBS for four consecutive weeks is shown. Arrow denotes collagen deposition in a peribronchovascular distribution. Data shown represent at least five mice from at least three separate experiments (40×). Bars, 100 μ m. (B) Quantification of collagen content using Sirius red colorimetric assay shows increased collagen deposition in the lungs of individual B6.AhR^{d/d} and B6.TCRδ^{-/-} ($\delta^{-/-}$) mice compared with WT C57BL/6 (wt) mice treated with *B. subtilis* or PBS for four consecutive weeks. The mean is shown as a solid line. Data were compiled from five individual mice from at least two separate experiments.

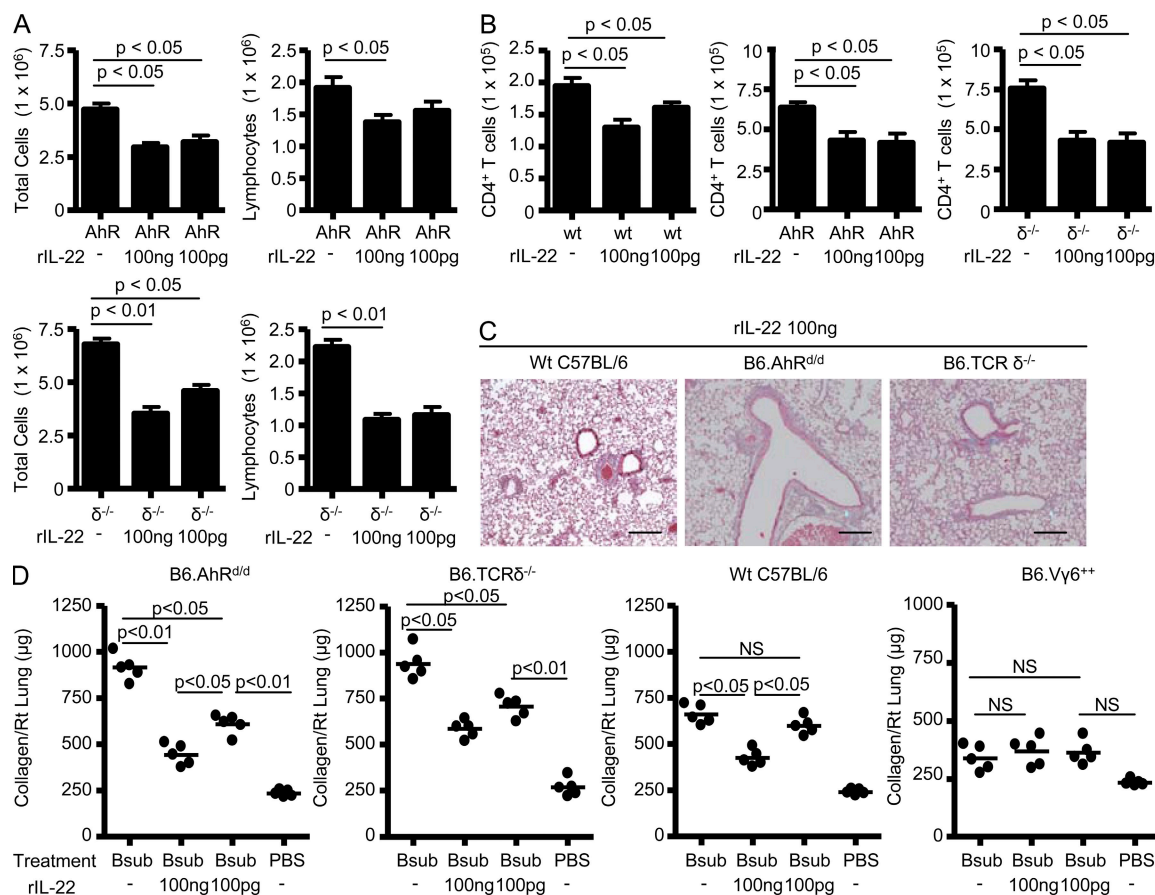


Figure 6. B6.AhR^{Δd} and B6.TCRδ^{-/-} mice treated with recombinant IL-22 have less lung inflammation and fibrosis. (A) Total and differential cell counts performed on lung homogenates from B6.AhR^{Δd} (AhR) and B6.TCRδ^{-/-} (δ^{-/-}) mice treated with a combination of recombinant IL-22 and *B. subtilis* or vehicle and *B. subtilis* for four consecutive weeks. Data were compiled from at least five mice per experiment from two separate experiments (mean ± SD). (B) Number of CD4⁺ T cells in the lung of WT C57BL/6 (wt), B6.AhR^{Δd} (AhR), and B6.TCRδ^{-/-} (δ^{-/-}) mice treated with a combination of recombinant IL-22 and *B. subtilis* or vehicle and *B. subtilis* for four consecutive weeks. Data were compiled from at least five mice per experiment from two separate experiments (mean ± SD). (C) Representative Masson's trichrome staining of lungs from B6.AhR^{Δd}, B6.TCRδ^{-/-}, and WT C57BL/6 mice repeatedly treated with *B. subtilis* and recombinant IL-22 for four consecutive weeks is shown. Data shown represent at least five mice from at least two separate experiments (40×). Bars, 100 μm. (D) Quantification of collagen content using Sirius red colorimetric assay in the lungs of individual B6.AhR^{Δd}, B6.TCRδ^{-/-}, WT C57BL/6, and B6.Vγ6^{+/+} mice compared with mice treated with *B. subtilis* or sterile PBS alone for four consecutive weeks is shown. The mean is shown as a solid line. Data were compiled from five individual mice from at least two separate experiments. NS, not significant. P > 0.05.

treatment of Vγ6^{+/+} mice with *B. subtilis* in combination with the AhR inhibitor resulted in decreased frequency of γδ T cells that express IL-22 compared with mice treated with *B. subtilis* and vehicle. In addition, the number of IL-22-expressing γδ T cells and the level of IL-22 in the lung were markedly reduced in Vγ6^{+/+} mice treated with the AhR inhibitor at both concentrations relative to mice treated with *B. subtilis* and vehicle (Fig. 7, B and C). With reduced IL-22 expression, lung inflammation was accelerated with increased total cells, whereas the number of γδ T cells was relatively unaffected in the lung of Vγ6^{+/+} mice treated with the AhR inhibitor compared with mice exposed to *B. subtilis* and vehicle (Fig. 7 D). CD4⁺ T cells, however, were markedly increased (more than threefold) in the lung of Vγ6^{+/+} mice treated with the AhR inhibitor compared with mice exposed to *B. subtilis* treated with vehicle alone (Fig. 7 D). In the presence

of increased numbers of CD4⁺ T cells, lung fibrosis was accelerated, as assessed by both Masson's trichrome staining and quantitatively by Sirius red colorimetric assay, with a twofold increase in collagen deposition in the lung of Vγ6^{+/+} mice treated with 10 mM CH-223191 compared with control mice treated in an identical manner with *B. subtilis* and vehicle (Fig. 7, E and F).

To directly determine if blocking IL-22 results in increased lung inflammation and fibrosis, we treated WT C57BL/6 and TCR-δ^{-/-} mice with anti-IL-22 mAb in combination with *B. subtilis* for 4 wk. Lung inflammation, as assessed by total cell numbers, was not significantly different between mice treated with the anti-IL-22 antibody compared with isotype controls (Fig. 8 A). In contrast to γδ T cells in the lung of WT C57BL/6 mice, which were unaltered by the addition of the anti-IL-22 antibody, CD4⁺ T cells were

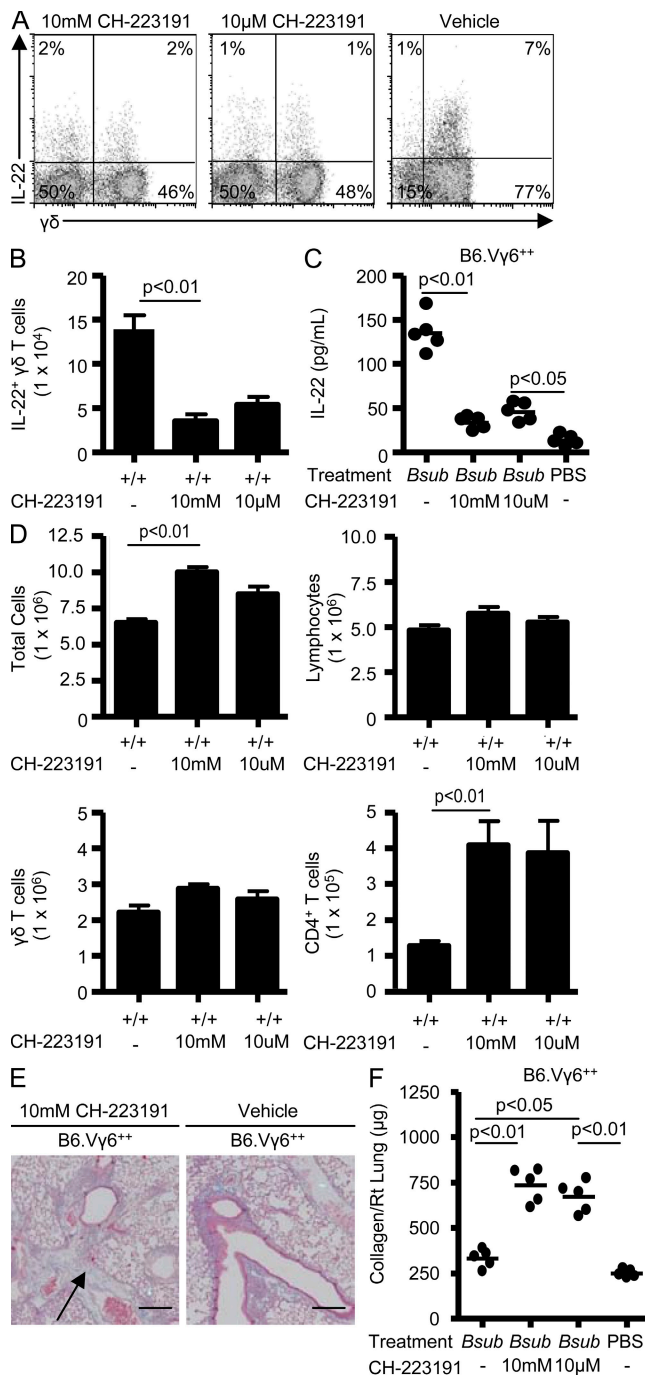


Figure 7. Acceleration of lung inflammation and fibrosis in transgenic Vγ6/Vδ1 mice treated with an AhR inhibitor. (A) Representative density plots of intracellular IL-22 expression in γδ T cells isolated from the lung of B6.Vγ6⁺ mice treated with the AhR inhibitor CH-223191 and *B. subtilis* or *B. subtilis* with vehicle for four consecutive weeks. γδ T cells expressing IL-22 were selected from a bivariate dot plot of CD3⁺/side scatter cells from the lymphocyte gate. The percentage of CD3⁺ T cells in each quadrant of the density plot is shown. Data are representative of at least five individual mice per experiment treated with CH-223191 at each concentration with *B. subtilis* from at least two separate experiments. (B) Number of IL-22-expressing γδ T cells in the lung of B6.Vγ6⁺ mice (+/+) treated with a combination of AhR inhibitor, CH-223191, and *B. subtilis* or

significantly increased in the lung of WT C57BL/6 mice treated with anti-IL-22 antibody compared with isotype control (Fig. 8 A). In the presence of an already exaggerated lung inflammatory response (Simonian et al., 2006), anti-IL-22 antibody had no effect on the recruitment of CD4⁺ T cells to the lung of TCR-δ^{-/-} mice (Fig. 8 A). As shown in Fig. 8 B, WT C57BL/6 mice treated with anti-IL-22 antibody had accelerated collagen deposition in the lung compared with mice treated in an identical fashion with an isotype control antibody. Exposure of TCR-δ^{-/-} mice to *B. subtilis* and anti-IL-22 antibody did not result in a further elevation of collagen deposition in the lung compared with mice treated with the isotype control (Fig. 8 B), likely because of the presence of significantly decreased IL-22 in the lung of TCR-δ^{-/-} mice relative to WT C57BL/6 mice (Fig. 1 D). Collectively, these data provide direct evidence that IL-22 regulates the accumulation of CD4⁺ T cells in the lung and *B. subtilis*-induced lung fibrosis.

CD4⁺ T cells promote lung fibrosis in response to *B. subtilis*

In the absence of γδ T cells, we have previously shown that an increased number of CD4⁺ T cells are recruited to the lung (Simonian et al., 2006). To determine whether the activation and differentiation state of CD4⁺ cells is affected by the presence or absence of IL-22-secreting Vγ6/Vδ1⁺ γδ T cells after *B. subtilis* exposure, we analyzed lung CD4⁺ T cells from WT C57BL/6, TCR-δ^{-/-}, and Vγ4^{-/-}/6^{-/-} mice. As compared with CD4⁺ T cells from WT C57BL/6 mice, a significantly increased percentage of CD4⁺ T lymphocytes from the lung of TCR-δ^{-/-} and Vγ4^{-/-}/6^{-/-} mice expressed high levels of CD44, a memory cell marker, and CD69, a marker of recent activation (Fig. 9 A). In addition, a reduced percentage of T cells expressed CD45RB, CD27, and CD62L, indicating that a larger fraction of CD4⁺ T cells in *B. subtilis*-treated TCR-δ^{-/-} and Vγ4^{-/-}/6^{-/-} mice had a

B. subtilis and vehicle for four consecutive weeks. Data were compiled from at least five mice per experiment from two separate experiments (mean ± SD). (C) IL-22 concentration in the lung of B6.Vγ6⁺ mice treated with a combination of AhR inhibitor, CH-223191, and *B. subtilis* or *B. subtilis* and vehicle for four consecutive weeks. The mean is shown as a solid line. Data were compiled from five individual mice from at least two separate experiments. (D) Number of cells in the lung of B6.Vγ6⁺ mice (+/+) treated with a combination of AhR inhibitor, CH-223191, and *B. subtilis* or *B. subtilis* and vehicle for four consecutive weeks. Data were compiled from at least five mice per experiment from two separate experiments (mean ± SD). (E) Representative Masson's trichrome staining of lungs from B6.Vγ6⁺ mice repeatedly treated with the AhR inhibitor, CH-223191, and *B. subtilis* compared with mice treated with *B. subtilis* and vehicle for four consecutive weeks is shown. Arrow denotes collagen deposition in a peribronchovascular distribution. Data shown represent at least five mice from at least two separate experiments (40×). Bars, 100 μm. (F) Quantification of collagen content using Sirius red colorimetric assay in the lungs of individual B6.Vγ6⁺ mice treated with the AhR inhibitor CH-223191 compared with mice treated with vehicle and *B. subtilis* or sterile PBS alone for four consecutive weeks is shown. The mean is shown as a solid line. Data were compiled from five individual mice from at least two separate experiments.

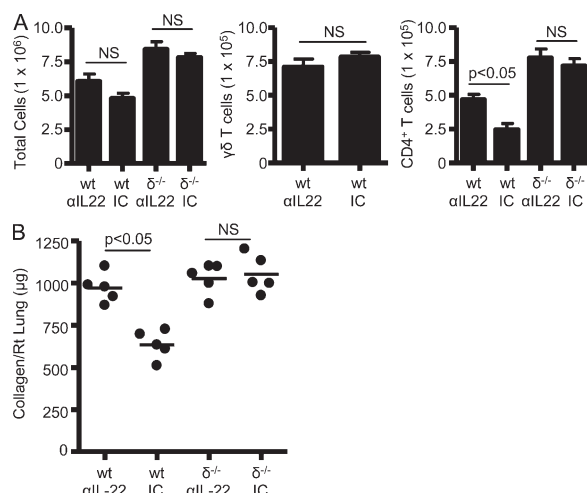


Figure 8. Administration of anti-IL-22 enhances the *B. subtilis*-induced CD4⁺ T cell alveolitis and accelerates lung fibrosis. (A) Total and differential cell counts performed on lung homogenates from WT C57BL/6 (wt) and B6.TCRδ^{-/-} (δ^{-/-}) mice treated with *B. subtilis* in combination with anti-IL-22 (αIL-22) or isotype control (IC) for 3 d a week for four consecutive weeks is shown. Data were compiled from at least five individual mice from two separate experiments (mean ± SD). (B) Quantification of collagen content using Sirius red colorimetric assay in the lungs of individual WT C57BL/6 (wt) and B6.TCRδ^{-/-} (δ^{-/-}) mice treated with *B. subtilis* in combination with anti-IL-22 (αIL-22) or isotype control (IC) for 3 d a week for four consecutive weeks is shown. The mean is shown as a solid line. Data represent five individual mice per experiment from two separate experiments. NS, not significant. P > 0.05.

highly activated effector phenotype, as compared with those from the lung of WT C57BL/6 mice (Fig. 9 A).

To test whether CD4⁺ T cells represent a pathogenic T cell subset and promote lung fibrosis in response to *B. subtilis*, we adoptively transferred CD4⁺ and CD8⁺ T cells from the spleen of naive WT C57BL/6 mice into TCR-β^{-/-}δ^{-/-} mice and subsequently treated them with *B. subtilis* by nasal inhalation. As shown in Fig. 9 B, mice receiving CD4⁺ T cells developed peribronchovascular mononuclear infiltrates similar to WT C57BL/6 mice treated in an identical fashion with *B. subtilis* (Fig. 9 B, top; Simonian et al., 2006, 2009a). Although CD4⁺ T cells were found in the lung and spleen of all mice reconstituted with CD4⁺ T lymphocytes, much higher numbers of CD4⁺ T cells were obtained after repeated exposure to *B. subtilis*, compared with similar mice treated with inhaled PBS. Conversely, TCR-β^{-/-}δ^{-/-} mice reconstituted with CD8⁺ T cells did not show a significant accumulation of cells in the lung after subsequent exposure to either *B. subtilis* or PBS by nasal inhalation (Fig. 9 B).

As opposed to CD8⁺ T cells, the adoptive transfer of CD4⁺ T cells into *B. subtilis*-treated TCR-β^{-/-}δ^{-/-} mice also resulted in lung fibrosis as detected by Masson trichrome (Fig. 9 B, bottom). In addition, quantification of collagen deposition by Sirius red colorimetric assay showed a 2.9-fold increase in collagen content in the lungs of these mice, as compared with CD4⁺ T cell-reconstituted control mice that were treated with PBS

by nasal inhalation (P < 0.01; Fig. 9 C). TCR-β^{-/-}δ^{-/-} mice reconstituted with CD8⁺ T cells also had a slight increase in collagen content in the lung when chronically exposed to *B. subtilis*, compared with PBS-treated CD8⁺ T cell-reconstituted control mice. However, similar levels of collagen deposition were seen in *B. subtilis*-treated TCR-β^{-/-}δ^{-/-} mice that were sham reconstituted by injecting sterile PBS into the tail vein (Fig. 9 C). Therefore, CD8⁺ T cells do not appear to have a significant role in the development of PF. Collectively, these data suggest that activated CD4⁺ T cells that accumulate in the lung in response to repeated *B. subtilis* exposure promote lung fibrosis.

rIL-22 reduces accumulation of CXCR3-expressing CD4⁺ T cells in the lung

Although Th1 cells typically express CXCR3, Th17 cells have also been shown to express this chemokine receptor (Acosta-Rodriguez et al., 2007). In addition, CXCR3 expression has been shown to be important in other models of lung injury/fibrosis such as bleomycin-induced lung fibrosis (Jiang et al., 2004). To determine if IL-22 affects CXCR3 expression on CD4⁺ T cells and recruitment of activated CD4⁺CXCR3⁺ T lymphocytes in the lung, we treated WT C57BL/6, Ahr^{d/d}, and TCR-δ^{-/-} mice with rIL-22 and *B. subtilis* for 4 wk. As shown in Fig. 10 (A and B), the percentage and number of CXCR3-expressing CD4⁺ T cells isolated from the lung of WT C57BL/6, Ahr^{d/d}, and TCR-δ^{-/-} mice treated with rIL-22 was significantly decreased compared with mice treated with *B. subtilis* and vehicle.

Next, we evaluated total lung homogenates from Vγ6^{+/+}, WT C57BL/6, and TCR-δ^{-/-} mice for the CXCR3 ligands CXCL9, 10, and 11. As shown in Fig. 10 C, levels of CXCL9 and CXCL10 were significantly increased in the lung of TCR-δ^{-/-} mice compared with Vγ6^{+/+} and WT C57BL/6 mice repeatedly exposed to *B. subtilis* over 4 wk, whereas CXCL11 was no different between the various strains of mice. To determine if exogenous rIL-22 could alter the levels of CXCR3 ligands in the lung, we treated WT C57BL/6, TCR-δ^{-/-}, and Ahr^{d/d} mice with *B. subtilis* and rIL-22 for 4 wk. As shown in Fig. 10 D, levels of CXCL9 were decreased in the lung of WT C57BL/6 mice treated with 100 ng rIL-22 but not at the lower dose. CXCL9 levels, however, were decreased in the lung of TCR-δ^{-/-} and Ahr^{d/d} mice at both concentrations of rIL-22 (Fig. 10 D). Levels of CXCL10 were not affected by treatment with rIL-22, suggesting that γδ T cells may affect CXCL10 expression independent of IL-22 (Fig. S3). Conversely, levels of CXCL9 were increased in the lung of Vγ6^{+/+} mice treated with *B. subtilis* for 4 wk in the presence of the AhR inhibitor CH-223191 (Fig. 10 E). Collectively, these data suggest that IL-22 alters the expression of the CXCR3 ligand CXCL9, resulting in a reduced recruitment of CD4⁺CXCR3⁺ T cells to the lung in response to repeated exposure to *B. subtilis*.

DISCUSSION

We developed a mouse model of HP to investigate the role of different T cell subsets in lung inflammation and fibrosis induced by chronic exposure to a common environmental

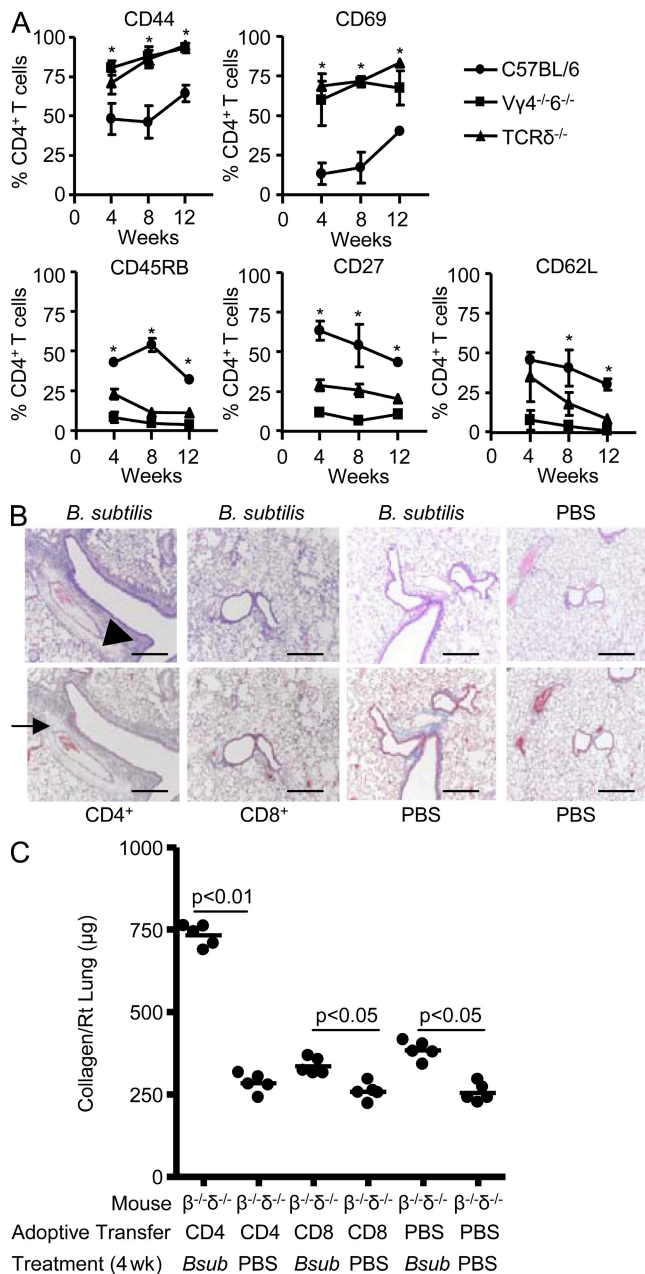


Figure 9. CD4⁺ T cells represent the pathogenic T cell subset and induce lung fibrosis. (A) Expression of CD44, CD69, CD45RB, CD27, and CD62L on CD4⁺ T cells isolated from the lungs of WT C57BL/6, TCR- $\delta^{-/-}$, and V $\gamma 4^{-/-}$ 6 $^{-/-}$ mice treated with *B. subtilis* for 4, 8, and 12 consecutive weeks is shown. Data represent the mean \pm SD of at least five mice at each time point treated with *B. subtilis* from at least two separate experiments. The asterisks denote a statistically significant ($P < 0.05$) difference in the percentage of CD4⁺ T cells that express each surface marker from the lung of WT C57BL/6 compared with TCR- $\delta^{-/-}$ mice treated with *B. subtilis* at each time point. (B) Representative H&E (top) and Masson trichrome (bottom) staining of lungs from TCR- $\beta^{-/-}$ $\delta^{-/-}$ mice reconstituted with either CD4⁺ or CD8⁺ T cells or sterile PBS followed by intranasal treatment with either *B. subtilis* or sterile PBS for four consecutive weeks is shown. Arrowhead denotes mononuclear infiltrates in the peribronchovascular space. Arrow denotes collagen deposition in a peribronchovascular distribution. Data represent at least four individual mice from at least two separate

microorganism, *B. subtilis* (Simonian et al., 2006). In this model, V $\gamma 6$ /V $\delta 1^{+}$ $\gamma\delta$ T cells expand in the lung in response to the microorganism and attenuate *B. subtilis*-induced lung inflammation and fibrosis (Simonian et al., 2006). In addition to IL-17A, the current study shows that V $\gamma 6$ /V $\delta 1^{+}$ $\gamma\delta$ T cells isolated from the lung of mice chronically exposed to *B. subtilis* express IL-22 and that expression of IL-22 is an important mechanism by which these T cells attenuate lung inflammation and fibrosis.

V $\gamma 6$ /V $\delta 1^{+}$ $\gamma\delta$ T cells are a rare population of $\gamma\delta$ T cells that normally reside in the female reproductive tract (Itoharu et al., 1990), tongue (Itoharu et al., 1990), and lung (Sim et al., 1994) but are rarely found in other tissues (Roark et al., 2004). Expansions of this TCR-invariant subset have been reported in the liver of *Listeria monocytogenes*-infected mice (Roark et al., 1996), testis during *Listeria*-induced orchitis (Mukasa et al., 1997), peritoneum of *Escherichia coli*-infected mice (Matsuzaki, Takada, and Nomoto, 1999), kidneys of mice infected intrarenally with *L. monocytogenes* (Ikebe et al., 2001), kidneys of rats treated with adriamycin (Ando et al., 2001), and brains of mice with experimental autoimmune encephalitis (Olive, 1995). In response to intratracheal *B. subtilis*, the lung $\gamma\delta$ T cell expansion is almost completely limited to the V $\gamma 6$ /V $\delta 1^{+}$ $\gamma\delta$ T cell subset and substantially exceeds that of both CD4⁺ and CD8⁺ $\alpha\beta$ -expressing T cells (Simonian et al., 2006, 2009a). As a result of its invariant TCR, it is likely that the TCR ligand for V $\gamma 6$ /V $\delta 1^{+}$ $\gamma\delta$ T cells is a host molecule whose expression is induced during inflammation. However, we and others have previously shown that live bacteria are required to induce a $\gamma\delta$ T cell response (Griffin et al., 1991; Boom et al., 1992; Skeen and Ziegler, 1993; Simonian et al., 2006).

Consistent with previous studies (Weaver et al., 2007; Veldhoen et al., 2008, 2009; Simonian et al., 2009a), we identified distinct populations of V $\gamma 6$ /V $\delta 1^{+}$ $\gamma\delta$ T cells that differentially express IL-17A and IL-22. In addition, IL-17A and IL-17F were also differentially expressed, with IL-22 expression identified as a subset of IL-17F-expressing V $\gamma 6$ /V $\delta 1^{+}$ $\gamma\delta$ T cells. These findings suggest that distinct V $\gamma 6$ /V $\delta 1^{+}$ $\gamma\delta$ T cell subsets may possess a range of functional capabilities. Recent data suggest that IL-17A and IL-17F may have complementary roles in host defense against *Staphylococcus aureus* (Ishigame et al., 2009). IL17a $^{-/-}$ IL17f $^{-/-}$ mice were more susceptible to mucocutaneous abscesses that contained *S. aureus* than either IL17a $^{-/-}$ or IL17f $^{-/-}$ mice, suggesting that *S. aureus* infection can be independently controlled by IL-17A or IL-17F (Ishigame et al., 2009). Although IL-17A and IL-17F bind to the same receptors, the binding affinities of IL-17A

experiments for H&E and Masson Trichrome staining (40 \times). Bars, 100 μ m. (C) Quantification of collagen content using Sirius Red by colorimetric assay in the lungs of individual TCR- $\beta^{-/-}$ $\delta^{-/-}$ ($\beta^{-/-}$ $\delta^{-/-}$) mice reconstituted with CD4⁺, CD8⁺, or sterile PBS by tail vein injection followed by repeated intranasal treatment with *B. subtilis* (*Bsub*) or sterile PBS for four consecutive weeks. The mean is shown as a solid line. Data were compiled from five individual mice from at least two separate experiments.

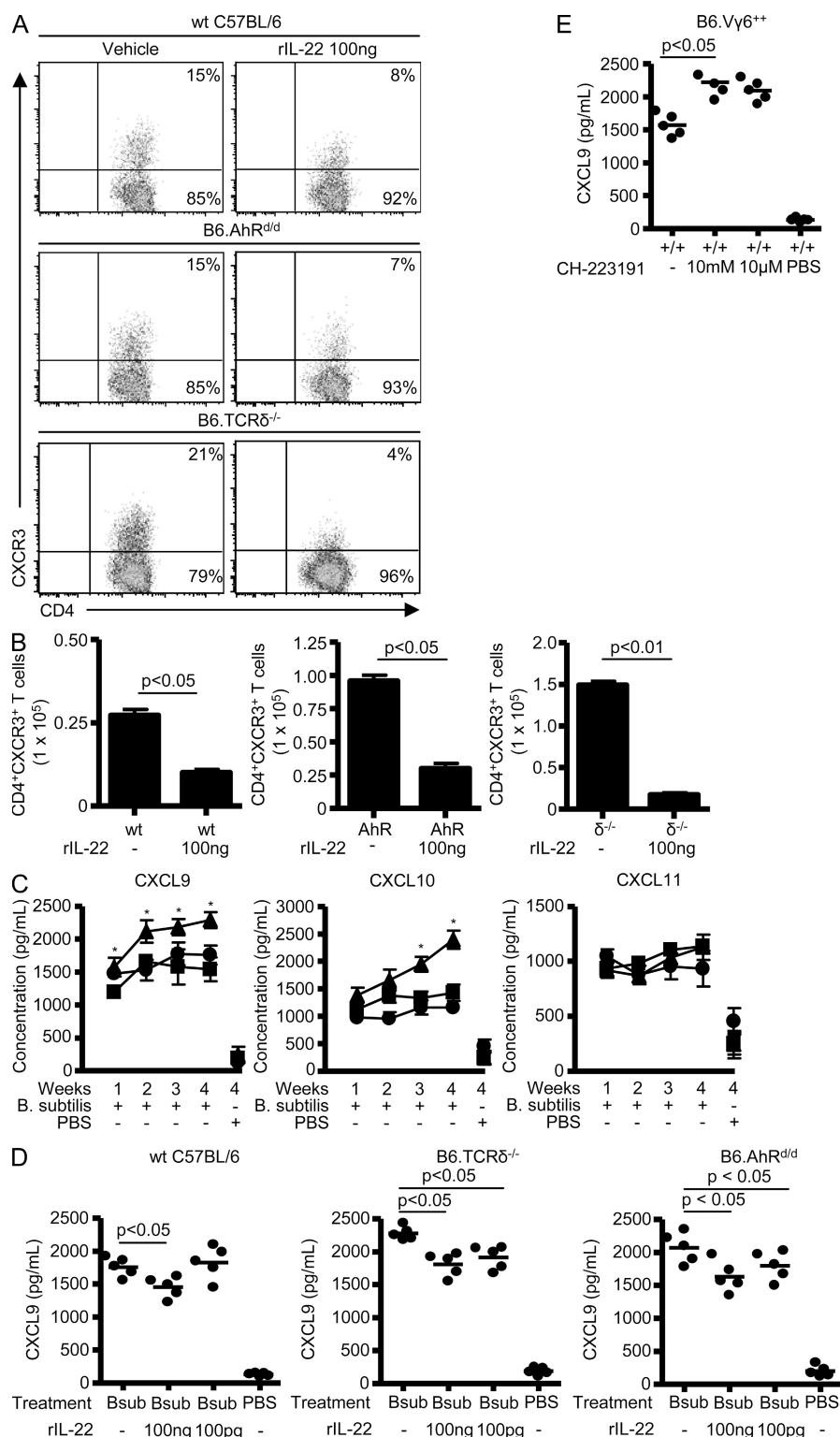


Figure 10. Recombinant IL-22 decreases CXCR3 expression by CD4⁺ T cells and levels of CXCL9 in the lung. (A) Representative density plots of CXCR3 expression by CD4⁺ T cells isolated from the lung of WT C57BL/6, B6.AhR^{Δd}, and B6.TCRδ^{-/-} mice treated with a combination of recombinant IL-22 and *B. subtilis* or vehicle and *B. subtilis* for four consecutive weeks. CD4⁺ T cells were selected from a bivariate dot plot of CD3⁺CD4⁺ cells from the lymphocyte gate. The percentage of CD3⁺CD4⁺ T cells expressing CXCR3 is shown in the top right quadrant of the density plot. Data represent at least five individual mice per experiment from two separate experiments. (B) Number of CXCR3-expressing CD4⁺ T cells in the lung of WT C57BL/6 (wt), B6.AhR^{Δd} (AhR), and B6.TCRδ^{-/-} (δ^{-/-}) mice treated with a combination of recombinant IL-22 and *B. subtilis* or vehicle and *B. subtilis* for four consecutive weeks. Data were compiled from at least five individual mice per experiment from two separate experiments. (C) Levels of CXCL9, 10, and 11 in the lung of WT C57BL/6 (●), B6.Vγ6^{+/+} (■), and B6.TCRδ^{-/-} (▲) mice treated with *B. subtilis* for four consecutive weeks compared with PBS control. The asterisks denote a statistically significant ($P < 0.05$) difference in lung chemokine concentration at each time point between B6.TCRδ^{-/-} and B6.Vγ6^{+/+} mice. Data were compiled from at least five individual mice at each time point from two separate experiments (mean ± SD). (D) Levels of CXCL9 in the lung of WT C57BL/6, TCRδ^{-/-}, and AhR^{Δd} mice treated with a combination of recombinant IL-22 and *B. subtilis*, *B. subtilis*, or PBS for four consecutive weeks. The mean is shown as a solid line. Data were compiled from five individual mice from two separate experiments. (E) Levels of CXCL9 in the lung of B6.Vγ6^{+/+} mice treated with a combination of the AhR inhibitor, CH-223191, and *B. subtilis*, *B. subtilis*, or PBS for four consecutive weeks. The mean is shown as a solid line. Data were compiled from five individual mice from two separate experiments.

and IL-17F for IL-17RA and IL-17RC may be different (Hymowitz et al., 2001; Kuestner et al., 2007; Wright et al., 2008). In mice, IL-17RA binds both IL-17A and IL-17F, but IL-17RC interacts with only IL-17F (Kuestner et al., 2007). Therefore, tissue distribution of the receptors for these cytokines

likely determines where they exert their functional capabilities (Gaffen, 2009). IL-17RA mRNA was shown to be highly expressed in lymphoid tissues such as the thymus, spleen, and lymph nodes, whereas IL-17RC mRNA was expressed in nonhematopoietic tissues such as the colon, small intestine, and lung (Ishigame et al., 2009), with IL-22

that express IL-22 and IL-17F may protect epithelial integrity in the lung through IL-22 receptor or IL-17RC signaling.

Because recent studies show that AhR signaling is important for IL-22 expression by $\alpha\beta$ - and $\gamma\delta$ -expressing T cells (Veldhoen et al., 2008; Martin et al., 2009), we analyzed and found substantial reductions in IL-22 levels in the lung of *B. subtilis*-treated AhR^{d/d} mice as well as reduced IL-22 expression by V γ 6/V δ 1⁺ $\gamma\delta$ T cells, whereas IL-17A and IL-17F expression was unaffected. With the reduction in IL-22 levels in the lung of *B. subtilis*-treated AhR^{d/d} mice, lung fibrosis was accelerated. The corroboration of these findings using an anti-IL-22 mAb suggests that IL-22 plays a critical role in regulating collagen deposition in the lung. We recently showed that in the absence of IL-17A receptor signaling, IL-17ra^{-/-} mice had delayed clearance of *B. subtilis* and increased lung inflammation and fibrosis (Simonian et al., 2009a). Conversely, despite reduced IL-22 expression, AhR^{d/d} mice chronically exposed to *B. subtilis* had no defects in bacterial clearance (Fig. S4), likely because of an unaffected IL-17A response. Although synergy between IL-17A and IL-22 cannot be excluded, these data support the concept that IL-17A-expressing V γ 6/V δ 1⁺ $\gamma\delta$ T cells promote microbial elimination, whereas the IL-22-expressing population limits lung inflammation and fibrosis. In the bleomycin model of lung inflammation and fibrosis, however, IL-17A is necessary for lung fibrosis either through IL-1 β (Wilson et al., 2010) or complex interactions that regulate IL-22 expression and function (Sonnenberg et al., 2010). In addition, IL-17A has been shown to be pathogenic in another model of HP induced by repeated exposure to *Saccharopolyspora rectivirgula* (Joshi et al., 2009; Simonian et al., 2009b). Therefore, whether IL-17A and IL-22 protect or promote lung inflammation and fibrosis is likely dependent on the inhaled agent.

IL-22 has emerged as an important cytokine in mucosal immunity (Aujla and Kolls, 2009). The mechanisms by which IL-22 protects epithelial structures in the lung, gut, and other organ systems from damage induced by numerous environmental insults are under intense investigation. Emerging data suggest that IL-22 may provide mucosal protection by inducing antimicrobial peptides from epithelial cells in the lung, gut, and skin as well as maintaining epithelial integrity either by preventing injury or accelerating epithelial repair after a variety of insults (Liang et al., 2006; Zheng et al., 2007, 2008; Aujla et al., 2008). In a mouse model of host defense against Gram-negative bacterial infection, WT mice given anti-IL-22 antibody before lung infection with *Klebsiella pneumoniae* had greater dissemination of infection and increased mortality than mice given a control antibody (Aujla et al., 2008). The combination of IL-17A and IL-22 significantly increased expression of an antimicrobial protein, lipocalin-2, in mouse tracheal epithelial cells, suggesting that IL-22 and IL-17A act synergistically, although IL-22 was shown to be more important for microbial elimination (Aujla et al., 2008). IL-22 was also found to induce clonogenic potential in human bronchial epithelial cells as well as enhanced recovery of epithelial resistance after epithelial injury (Aujla et al., 2008). In the *B. subtilis* model,

however, we found increased numbers of activated CD4⁺ T cells in the lung of mice deficient in IL-22-expressing V γ 6/V δ 1⁺ $\gamma\delta$ T cells and accelerated lung fibrosis. Upon treatment with recombinant IL-22, AhR^{d/d} and TCR- δ ^{-/-} mice not only had reduced collagen deposition but also a diminished CD4⁺ T cell alveolitis. Conversely, transgenic V γ 6^{+/+} mice treated with the AhR inhibitor CH-23191 had decreased levels of IL-22 and increased numbers of CD4⁺ T cells in the lung that resulted in loss of protection against *B. subtilis*-induced lung fibrosis. In addition, neutralization of IL-22 by treatment with an anti-IL-22 mAb resulted in elevated numbers of CD4⁺ T cells and acceleration of lung fibrosis. Adoptive transfer of CD4⁺ T cells into mice deficient in both $\alpha\beta$ and $\gamma\delta$ T cells resulted in collagen deposition in the lung, further implicating CD4⁺ T lymphocytes in the pathogenesis of *B. subtilis*-induced lung fibrosis.

Th17 cytokines induce numerous chemokines and growth factors to promote cellular recruitment to the site of injury (for review see Alcorn et al., 2010). In the absence of $\gamma\delta$ T cells and the resultant diminution in IL-22 expression in our model, the lungs of *B. subtilis*-treated TCR- δ ^{-/-} mice contain a significantly greater number of CD4⁺CXCR3⁺ T cells that express an activated effector phenotype as compared with WT C57BL/6 mice. The diminished CD4⁺CXCR3⁺ T cell inflammatory response in WT C57BL/6, TCR- δ ^{-/-}, and AhR^{d/d} mice as a result of exogenous rIL-22 administration suggests that the mechanism by which IL-22 decreases CD4⁺ T cell recruitment to lung in response to *B. subtilis* is through decreased expression of CXCR3 ligands. Consistent with this observation, levels of the CXCR3 ligand CXCL9 were decreased in the lung of both AhR^{d/d} and TCR- δ ^{-/-} mice in response to rIL-22. Because the IL-22 receptor and expression of CXCL9 have been demonstrated on lung epithelial cells (Aujla et al., 2008), rIL-22 may decrease expression of CXCL9 by lung epithelial cells that limit the recruitment of CD4⁺CXCR3⁺ T cells to the lung in response to repeated exposure to *B. subtilis*.

The fact that lung fibrosis was not completely abrogated in AhR^{d/d} and TCR- δ ^{-/-} mice treated with rIL-22 raises the possibility that either higher levels of IL-22 in lung are required or other factors expressed by $\gamma\delta$ T cells are necessary to further reduce collagen deposition in the lung. Therefore, IL-17A, IL-17F, or other factors expressed by V γ 6/V δ 1⁺ $\gamma\delta$ T cells may still act synergistically with IL-22 to reduce CD4⁺ T cell recruitment to the lung and, thus, lung fibrosis. However, the presence of an exaggerated *B. subtilis*-induced fibrotic response in AhR^{d/d} and TCR- δ ^{-/-} mice, despite high levels of IL-17A and IL-17F in the lung, strongly suggests that IL-22 is the more critical Th17 cytokine for protecting against lung fibrosis induced by chronic exposure to *B. subtilis*.

Although cessation of antigen exposure often improves lung inflammation, irreversible PF still develops in ~41% of HP subjects and is associated with increased morbidity and mortality (Vourlekis et al., 2004). Current therapeutic options for HP patients are limited to corticosteroids which nonspecifically suppress T cell function. The ability of rIL-22 to regulate

PF in mice raises the possibility that immunotherapy directed toward increasing IL-22 levels in the lung may be beneficial in diseases characterized by chronic lung inflammation.

MATERIALS AND METHODS

Treatment of mice. 8-wk-old C57BL/6, TCR- $\delta^{-/-}$, TCR- $\beta^{-/-}\delta^{-/-}$, and AhR^{d/d} mice (The Jackson Laboratory) and transgenic V γ 6^{+/+} (Sim et al., 1995; Roark et al., 2004) and V γ 4^{-/-}6^{-/-} (Simonian et al., 2006) mice were treated with 30 μ l (5 million CFU) *B. subtilis* (American Type Culture Collection) or sterile PBS on three consecutive days each week for up to four consecutive weeks by nasal inhalation. All mice have been backcrossed onto a C57BL/6 background for at least 10 generations. *B. subtilis* was prepared as previously described (Simonian et al., 2006). A limulus amebocyte assay (Sigma-Aldrich) confirmed that the *B. subtilis* preparation and sterile PBS contained <20 μ g of endotoxin/ml. For all experiments using 100 ng or 100 pg of mouse rIL-22 (R&D Systems) or 10 mM or 10 μ M of the AhR inhibitor CH-223191 (EMD), mice were given IL-22 or CH-223191 by nasal inhalation in combination with *B. subtilis* for three consecutive days each week for four consecutive weeks. IL-22 was dissolved in PBS with 1% BSA, whereas CH-223191 is dissolved in DMSO. Therefore, PBS with 1% BSA and DMSO were used as vehicle controls. For experiments involving anti-IL22 mAb, mice were treated with *B. subtilis* in combination with 1 μ g of either anti-IL-22 or isotype control mAb (R&D Systems) for 3 d a week for four consecutive weeks. On the other 4 d of the week, mice were treated with either anti-IL-22 or isotype control mAb suspended in sterile PBS. Mice were lightly anesthetized with isoflurane to allow inhalation of either *B. subtilis* or sterile PBS. These studies were approved by the Animal Care and Use Committee at the University of Colorado Denver.

Preparation of mononuclear cells from lung homogenates. Mice were sacrificed 24 h after the last treatment with *B. subtilis* as previously described (Simonian et al., 2006). The right lung was removed, snap-frozen in liquid nitrogen, and stored at -80°C for collagen quantification after sterile PBS was infused through the pulmonary vasculature by right heart puncture to remove any contaminating peripheral blood mononuclear cells. The left lung was digested with collagenase (Sigma-Aldrich) and DNase (Boehringer Mannheim). The collagenase-digested lungs were layered on top of Ficoll (Accurate Chemical & Scientific Corporation) and centrifuged at 1,200 rpm for 30 min at room temperature. The interface between the medium and Ficoll was removed and washed twice with RPMI 1640 containing 5% FBS.

Flow cytometry and immunofluorescence analysis. T cells isolated from the lungs of mice treated with either *B. subtilis* or sterile PBS were surface stained with mAbs directed against CD3 (PECy7; BD), CD4 (Alexa Fluor 405; BD), C δ (FITC; BD), CXCR3 (APC; eBioscience), CD44 (APC; eBioscience), CD45RB (PE; eBioscience), CD27 (APC; eBioscience), CD62L (PECy5.5; eBioscience), and CD69 (PECy5.5; eBioscience). For intracellular cytokine staining, total lung cells were cultured at 10^6 cells/ml in complete RPMI media containing 10 μ g/ml brefeldin A (Sigma-Aldrich) at 37°C for 4 h. The cells were washed and stained with mAbs directed against CD3 (PerCP; BD), CD4 (FITC; BD), and C δ (FITC; BD), followed by fixation in 1% paraformaldehyde overnight. $\gamma\delta$ T cells that express the V γ 6⁺ TCR were identified using 17D1 mAb (Roark et al., 2004). Fixed cells were permeabilized in 0.5% saponin and stained with IL-17A (APC; eBioscience), IL-22 (PE; R&D Systems), and IL-17F (APC or PE; R&D Systems) mAbs and isotype controls for 30 min at 4°C . The lymphocyte population was identified using forward and 90° light scatter patterns, and fluorescence intensity was analyzed using a FACSAria cytometer (BD). The data files were analyzed using FlowJo software (Tree Star, Inc.).

Histology. Mice were sacrificed 24 h after their last exposure to *B. subtilis* or sterile PBS. The lungs were removed and infused with 10% formalin, embedded in paraffin, and stained with hematoxylin and eosin (H&E) and Masson Trichrome (Sigma-Aldrich) according to the manufacturer's instructions.

Cytokine analysis and collagen quantification. Total lung homogenates were prepared by homogenizing whole lung samples in 500 μ l of sterile PBS from each group of mice treated with either *B. subtilis* or sterile PBS for four consecutive weeks. 100 μ l of supernatant from each lung homogenate was analyzed for cytokines by ELISA for IL-17A (eBioscience), IL-17F, IL-22, CXCL9, CXCL10, and CXCL11 (R&D Systems) according to the manufacturer's instructions. The collagen content of the right lung was determined using Sirius Red staining as previously described (Simonian et al., 2006).

Total and differential cell counts. Total and differential cell counts were performed on collagenase-digested lung before purification of mononuclear cells over Ficoll as previously described (Simonian et al., 2006, 2009b). In brief, single-cell suspensions of total lung cells were transferred to a glass slide using a cytocentrifuge apparatus and stained with Wright and Giemsa per manufacturer's instructions. Epithelial cells were not included in the total cell count and RBCs were removed by RBC lysis. Differential cell counts were performed by counting at least 400 cells under a high power field.

Adoptive transfer experiments. CD4⁺ and CD8⁺ T cells were isolated from spleens of untreated C57BL/6 mice and purified by MACS (Miltenyi Biotec) using negative selection for either CD4⁺ or CD8⁺ T lymphocytes. Flow cytometry confirmed >95% purity for each T cell population before adoptive transfer of 5×10^5 cells/100 μ l of sterile PBS by tail vein injection into TCR- $\beta^{-/-}\delta^{-/-}$ mice. In brief, total splenocytes were obtained by pushing spleens through a 70- μ m pore-size mesh (Falcon) with subsequent resuspension in RBC lysis buffer (eBioscience). Cells were resuspended in buffer and biotinylated antibody cocktail, mixed, and incubated at 4°C for 10 min. Anti-biotin microbeads were added per the manufacturer's instructions, mixed, and incubated for 15 min at 4°C . The cells were washed and applied to the column per the manufacturer's instructions. The effluent, which contained the unlabeled CD4⁺ or CD8⁺ T cells, was collected and passed over a second column to further enrich each T cell population. Cell counts for CD4⁺ and CD8⁺ T lymphocytes were determined by Coulter counter (Beckman Coulter).

Statistical analysis. A Mann-Whitney *U* analysis and one-way ANOVA with a Bonferroni's multiple comparison test were used to determine whether there were significant differences between the treatment groups at each time point (Prism 4; GraphPad Software). $P < 0.05$ was considered statistically significant.

Online supplemental material. Fig. S1 demonstrates that IL-17A and IL-22 are not expressed by $\gamma\delta$ T cells isolated from the spleen of homozygous transgenic V γ 6/V δ 1 (B6.V γ 6^{+/+}) mice repeatedly exposed to *B. subtilis*. Fig. S2 shows that recombinant IL-22 does not decrease levels of CXCL10 in the lung. Fig. S3 demonstrates the absence of an effect of rIL-22 on CXCL10 levels in the lung of TCR- $\delta^{-/-}$ mice. Fig. S4 demonstrates similar clearance of *B. subtilis* from the lung of AhR^{d/d} and WT C57BL/6 mice. Online supplemental material is available at <http://www.jem.org/cgi/content/full/jem.20100061/DC1>.

This work is supported by the following National Institutes of Health grants: HL062410 and ES011810 (to A.P. Fontenot) and HL089766 (to P.L. Simonian).

The authors have no competing financial interests.

Submitted: 8 January 2010

Accepted: 30 August 2010

REFERENCES

- Acosta-Rodriguez, E.V., L. Rivino, J. Geginat, D. Jarrossay, M. Gattorno, A. Lanzavecchia, F. Sallusto, and G. Napolitani. 2007. Surface phenotype and antigenic specificity of human interleukin 17-producing T helper memory cells. *Nat. Immunol.* 8:639–646. doi:10.1038/ni1467
- Alcorn, J.F., C.R. Crowe, and J.K. Kolls. 2010. TH17 cells in asthma and COPD. *Annu. Rev. Physiol.* 72:495–516. doi:10.1146/annurev-physiol-021909-135926
- Ando, T., H. Wu, D. Watson, T. Hirano, H. Hirakata, M. Fujishima, and J.F. Knight. 2001. Infiltration of canonical Vgamma4/Vdelta1

- gammadelta T cells in an adriamycin-induced progressive renal failure model. *J. Immunol.* 167:3740–3745.
- Aujla, S.J., and J.K. Kolls. 2009. IL-22: a critical mediator in mucosal host defense. *J. Mol. Med.* 87:451–454. doi:10.1007/s00109-009-0448-1
- Aujla, S.J., Y.R. Chan, M. Zheng, M. Fei, D.J. Askew, D.A. Pociask, T.A. Reinhart, F. McAllister, J. Edeal, K. Gaus, et al. 2008. IL-22 mediates mucosal host defense against Gram-negative bacterial pneumonia. *Nat. Med.* 14:275–281. doi:10.1038/nm1710
- Barrera, L., F. Mendoza, J. Zúñiga, A. Estrada, A.C. Zamora, E.I. Melendro, R. Ramírez, A. Pardo, and M. Selman. 2008. Functional diversity of T-cell subpopulations in subacute and chronic hypersensitivity pneumonitis. *Am. J. Respir. Crit. Care Med.* 177:44–55. doi:10.1164/rccm.200701-093OC
- Boom, W.H., K.A. Chervenak, M.A. Mincek, and J.J. Ellner. 1992. Role of the mononuclear phagocyte as an antigen-presenting cell for human $\gamma\delta$ T cells activated by live *Mycobacterium tuberculosis*. *Infect. Immun.* 60:3480–3488.
- Born, W.K., N. Jin, M.K. Aydintug, J.M. Wands, J.D. French, C.L. Roark, and R.L. O'Brien. 2007. gammadelta T lymphocytes-selectable cells within the innate system? *J. Clin. Immunol.* 27:133–144. doi:10.1007/s10875-007-9077-z
- Bourke, S.J., S.W. Banham, R. Carter, P. Lynch, and G. Boyd. 1989. Longitudinal course of extrinsic allergic alveolitis in pigeon breeders. *Thorax*. 44:415–418. doi:10.1136/thx.44.5.415
- Gaffen, S.L. 2009. Structure and signalling in the IL-17 receptor family. *Nat. Rev. Immunol.* 9:556–567. doi:10.1038/nri2586
- Griffin, J.P., K.V. Harshan, W.K. Born, and I.M. Orme. 1991. Kinetics of accumulation of $\gamma\delta$ receptor-bearing T lymphocytes in mice infected with live mycobacteria. *Infect. Immun.* 59:4263–4265.
- Hymowitz, S.G., E.H. Filvaroff, J.P. Yin, J. Lee, L. Cai, P. Risser, M. Maruoka, W. Mao, J. Foster, R.F. Kelley, et al. 2001. IL-17s adopt a cystine knot fold: structure and activity of a novel cytokine, IL-17F, and implications for receptor binding. *EMBO J.* 20:5332–5341. doi:10.1093/emboj/20.19.5332
- Ikebe, H., H. Yamada, M. Nomoto, H. Takimoto, T. Nakamura, K.H. Sonoda, and K. Nomoto. 2001. Persistent infection with *Listeria monocytogenes* in the kidney induces anti-inflammatory invariant fetal-type gammadelta T cells. *Immunology*. 102:94–102. doi:10.1046/j.1365-2567.2001.01149.x
- Ishigame, H., S. Sakuta, T. Nagai, M. Kadoki, A. Nambu, Y. Komiyama, N. Fujikado, Y. Tanahashi, A. Akitsu, H. Kotaki, et al. 2009. Differential roles of interleukin-17A and -17F in host defense against mucocutaneous bacterial infection and allergic responses. *Immunity*. 30:108–119. doi:10.1016/j.immuni.2008.11.009
- Itoharu, S., A.G. Farr, J.J. Lafaille, M. Bonneville, Y. Takagaki, W. Haas, and S. Tonegawa. 1990. Homing of a $\gamma\delta$ thymocyte subset with homogeneous T-cell receptors to mucosal epithelia. *Nature*. 343:754–757. doi:10.1038/343754a0
- Jiang, D., J. Liang, J. Hodge, B. Lu, Z. Zhu, S. Yu, J. Fan, Y. Gao, Z. Yin, R. Homer, et al. 2004. Regulation of pulmonary fibrosis by chemokine receptor CXCR3. *J. Clin. Invest.* 114:291–299.
- Joshi, A.D., D.J. Fong, S.R. Oak, G. Trujillo, K.R. Flaherty, F.J. Martinez, and C.M. Hogaboam. 2009. Interleukin-17-mediated immunopathogenesis in experimental hypersensitivity pneumonitis. *Am. J. Respir. Crit. Care Med.* 179:705–716. doi:10.1164/rccm.200811-1700OC
- Kim, S.H., E.C. Henry, D.K. Kim, Y.H. Kim, K.J. Shin, M.S. Han, T.G. Lee, J.K. Kang, T.A. Gasiewicz, S.H. Ryu, and P.G. Suh. 2006. Novel compound 2-methyl-2H-pyrazole-3-carboxylic acid (2-methyl-4-*o*-tolylazo-phenyl)-amide (CH-223191) prevents 2,3,7,8-TCDD-induced toxicity by antagonizing the aryl hydrocarbon receptor. *Mol. Pharmacol.* 69:1871–1878. doi:10.1124/mol.105.021832
- Kuestner, R.E., D.W. Taft, A. Haran, C.S. Brandt, T. Brender, K. Lum, B. Harder, S. Okada, C.D. Ostrander, J.L. Kreindler, et al. 2007. Identification of the IL-17 receptor related molecule IL-17RC as the receptor for IL-17F. *J. Immunol.* 179:5462–5473.
- Lalancette, M., G. Carrier, M. Laviolette, S. Ferland, J. Rodrique, R. Bégin, A. Cantin, and Y. Cormier. 1993. Farmer's lung. Long-term outcome and lack of predictive value of bronchoalveolar lavage fibrosing factors. *Am. Rev. Respir. Dis.* 148:216–221.
- Liang, S.C., X.Y. Tan, D.P. Luxenberg, R. Karim, K. Dunussi-Joannopoulos, M. Collins, and L.A. Fouser. 2006. Interleukin (IL)-22 and IL-17 are coexpressed by Th17 cells and cooperatively enhance expression of antimicrobial peptides. *J. Exp. Med.* 203:2271–2279. doi:10.1084/jem.20061308
- Luzina, I.G., N.W. Todd, A.T. Iacono, and S.P. Atamas. 2008. Roles of T lymphocytes in pulmonary fibrosis. *J. Leukoc. Biol.* 83:237–244. doi:10.1189/jlb.0707504
- Martin, B., K. Hirota, D.J. Cua, B. Stockinger, and M. Veldhoen. 2009. Interleukin-17-producing gammadelta T cells selectively expand in response to pathogen products and environmental signals. *Immunity*. 31:321–330. doi:10.1016/j.immuni.2009.06.020
- Matsuzaki, G., H. Takada, and K. Nomoto. 1999. *Escherichia coli* infection induces only fetal thymus-derived $\gamma\delta$ T cells at the infected site. *Eur. J. Immunol.* 29:3877–3886. doi:10.1002/(SICI)1521-4141(199912)29:12<3877::AID-IMMU3877>3.0.CO;2-C
- Mönkäre, S., and T. Haahela. 1987. Farmer's lung—a 5-year follow-up of eighty-six patients. *Clin. Allergy*. 17:143–151. doi:10.1111/j.1365-2222.1987.tb02332.x
- Mukasa, A., M. Lahn, E.K. Pflum, W. Born, and R.L. O'Brien. 1997. Evidence that the same $\gamma\delta$ T cells respond during infection-induced and autoimmune inflammation. *J. Immunol.* 159:5787–5794.
- Nanno, M., T. Shiohara, H. Yamamoto, K. Kawakami, and H. Ishikawa. 2007. gammadelta T cells: firefighters or fire boosters in the front lines of inflammatory responses. *Immunol. Rev.* 215:103–113. doi:10.1111/j.1600-065X.2006.00474.x
- Okey, A.B., L.M. Vella, and P.A. Harper. 1989. Detection and characterization of a low affinity form of cytosolic Ah receptor in livers of mice non-responsive to induction of cytochrome P1-450 by 3-methylcholanthrene. *Mol. Pharmacol.* 35:823–830.
- Olive, C. 1995. $\gamma\delta$ T cell receptor variable region usage during the development of experimental allergic encephalomyelitis. *J. Neuroimmunol.* 62:1–7. doi:10.1016/0165-5728(95)00081-C
- Roark, C.E., M.K. Vollmer, P.A. Campbell, W.K. Born, and R.L. O'Brien. 1996. Response of a $\gamma\delta$ T cell receptor invariant subset during bacterial infection. *J. Immunol.* 156:2214–2220.
- Roark, C.L., M.K. Aydintug, J. Lewis, X. Yin, M. Lahn, Y.S. Hahn, W.K. Born, R.E. Tigelaar, and R.L. O'Brien. 2004. Subset-specific, uniform activation among V γ 6/V δ 1+ $\gamma\delta$ T cells elicited by inflammation. *J. Leukoc. Biol.* 75:68–75. doi:10.1189/jlb.0703326
- Selman, M. 2003. Hypersensitivity pneumonitis. In *Interstitial lung disease*. M.I. Schwarz and T.E. King, Jr., editors. B.C. Decker, Hamilton, Ontario. 452–484.
- Sim, G.K., R. Rajaserkar, M. Dessing, and A. Augustin. 1994. Homing and in situ differentiation of resident pulmonary lymphocytes. *Int. Immunol.* 6:1287–1295. doi:10.1093/intimm/6.9.1287
- Sim, G.K., C. Olsson, and A. Augustin. 1995. Commitment and maintenance of the $\alpha\beta$ and $\gamma\delta$ T cell lineages. *J. Immunol.* 154:5821–5831.
- Simonian, P.L., C.L. Roark, F. Diaz del Valle, B.E. Palmer, I.S. Douglas, K. Ikuta, W.K. Born, R.L. O'Brien, and A.P. Fontenot. 2006. Regulatory role of $\gamma\delta$ T cells in the recruitment of CD4⁺ and CD8⁺ T cells to lung and subsequent pulmonary fibrosis. *J. Immunol.* 177:4436–4443.
- Simonian, P.L., C.L. Roark, F. Wehrmann, A.M. Lanham, W.K. Born, R.L. O'Brien, and A.P. Fontenot. 2009a. IL-17A-expressing T cells are essential for bacterial clearance in a murine model of hypersensitivity pneumonitis. *J. Immunol.* 182:6540–6549. doi:10.4049/jimmunol.0900013
- Simonian, P.L., C.L. Roark, F. Wehrmann, A.K. Lanham, F. Diaz del Valle, W.K. Born, R.L. O'Brien, and A.P. Fontenot. 2009b. Th17-polarized immune response in a murine model of hypersensitivity pneumonitis and lung fibrosis. *J. Immunol.* 182:657–665. doi:10.4049/jimmunol.0900013
- Skeen, M.J., and H.K. Ziegler. 1993. Induction of murine peritoneal $\gamma\delta$ T cells and their role in resistance to bacterial infection. *J. Exp. Med.* 178:971–984. doi:10.1084/jem.178.3.971
- Sonnenberg, G.F., M.G. Nair, T.J. Kirn, C. Zaph, L.A. Fouser, and D. Artis. 2010. Pathological versus protective functions of IL-22 in airway inflammation are regulated by IL-17A. *J. Exp. Med.* 207:1293–1305. doi:10.1084/jem.20092054
- Veldhoen, M., K. Hirota, A.M. Westendorf, J. Buer, L. Dumoutier, J.C. Renaud, and B. Stockinger. 2008. The aryl hydrocarbon receptor links

- TH17-cell-mediated autoimmunity to environmental toxins. *Nature*. 453:106–109. doi:10.1038/nature06881
- Veldhoen, M., K. Hirota, J. Christensen, A. O'Garra, and B. Stockinger. 2009. Natural agonists for aryl hydrocarbon receptor in culture medium are essential for optimal differentiation of Th17 T cells. *J. Exp. Med.* 206:43–49. doi:10.1084/jem.20081438
- Vourlekis, J.S., M.I. Schwarz, R.M. Cherniack, D. Curran-Everett, C.D. Cool, R.M. Tudor, T.E. King Jr., and K.K. Brown. 2004. The effect of pulmonary fibrosis on survival in patients with hypersensitivity pneumonitis. *Am. J. Med.* 116:662–668. doi:10.1016/j.amjmed.2003.12.030
- Wands, J.M., C.L. Roark, M.K. Aydintug, N. Jin, Y.S. Hahn, L. Cook, X. Yin, J. Dal Porto, M. Lahn, D.M. Hyde, et al. 2005. Distribution and leukocyte contacts of gammadelta T cells in the lung. *J. Leukoc. Biol.* 78:1086–1096. doi:10.1189/jlb.0505244
- Weaver, C.T., R.D. Hatton, P.R. Mangan, and L.E. Harrington. 2007. IL-17 family cytokines and the expanding diversity of effector T cell lineages. *Annu. Rev. Immunol.* 25:821–852. doi:10.1146/annurev.immunol.25.022106.141557
- Wilson, M.S., S.K. Madala, T.R. Ramalingam, B.R. Gochuico, I.O. Rosas, A.W. Cheever, and T.A. Wynn. 2010. Bleomycin and IL-1 β -mediated pulmonary fibrosis is IL-17A dependent. *J. Exp. Med.* 207:535–552. doi:10.1084/jem.20092121
- Wright, J.F., F. Bennett, B. Li, J. Brooks, D.P. Luxenberg, M.J. Whitters, K.N. Tomkinson, L.J. Fitz, N.M. Wolfman, M. Collins, et al. 2008. The human IL-17F/IL-17A heterodimeric cytokine signals through the IL-17RA/IL-17RC receptor complex. *J. Immunol.* 181:2799–2805.
- Yoshizawa, Y., Y. Ohtani, H. Hayakawa, A. Sato, M. Suga, and M. Ando. 1999. Chronic hypersensitivity pneumonitis in Japan: a nationwide epidemiologic survey. *J. Allergy Clin. Immunol.* 103:315–320. doi:10.1016/S0091-6749(99)70507-5
- Zheng, Y., D.M. Danilenko, P. Valdez, I. Kasman, J. Eastham-Anderson, J. Wu, and W. Ouyang. 2007. Interleukin-22, a T_H17 cytokine, mediates IL-23-induced dermal inflammation and acanthosis. *Nature*. 445:648–651. doi:10.1038/nature05505
- Zheng, Y., P.A. Valdez, D.M. Danilenko, Y. Hu, S.M. Sa, Q. Gong, A.R. Abbas, Z. Modrusan, N. Ghilardi, F.J. de Sauvage, and W. Ouyang. 2008. Interleukin-22 mediates early host defense against attaching and effacing bacterial pathogens. *Nat. Med.* 14:282–289. doi:10.1038/nm1720